Master Thesis

FABRICATION AND CHARACTERIZATION OF NANOPARTICLES/PMMA ELECTROSPUN NANOFIBER MEMBRANES

Erasmus Mundus Master in Membrane Engineering

Magdalena Malankowska

Supervisor: Silvia Irusta

Zaragoza, 18.06.2013

Abstract

Currently, one of the most serious problems is to maintain the water balance in terms of quality and quantity. In recent times, membrane technology is considered to be essential as it ensures high water quality with low cost and maintenance of sustainable water resources. In this work different membranes were fabricated by electrospinning technique. PMMA (polymethyl methacrylate) was used as a base polymer material and the silver nanoparticles, silver nanowires or titanium dioxide were incorporated into the matrix. The aim was to produce polymeric membranes containing nanoparticles, fabricated by electrospinning in order to obtain the highest bactericidal effect for water treatment. The bactericidal effect was observed for three kinds of membranes however, the best results were obtained by the silver nanoparticles membrane with the *in situ* manufacturing method. The distribution of the nanoparticles in this membrane resulted more uniform, the size of the nanoparticles was smaller and the texture was the most mechanically resistant.

Acknowledgments:

I would like to thank the EM3E master and Reyes Mallada as a coordinator for the opportunity of developing my scientific skills and participating in the program, University of Zaragoza, Jesus Santamaria and all the INA group for the possibility of developing the project, supplying all of the required devices, Silvia Irusta for supervising me and giving essential advices and Ivan Moreno for help with the equipments and scientific support.

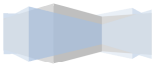

EN: The EM3E education programme has been funded with support from the European Commission. This publication reflects the views only of the author, and the Commission cannot be held responsible for any use which may be made of the information contained therein. Translation of this phrase in all EU languages.

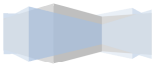

List of tables:

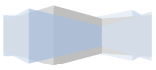

List of figures:

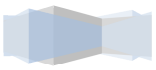

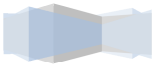

Table of content:

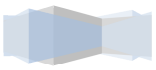

1. Introduction

The Nobel Laureate Richard P. Feynmann on the 29th of December 1959 at the California Institute of Technology gave a lecture at the annual meeting of the American Physical Society. The title of the lecture was: “There’s plenty of room at the bottom”, and it became the beginning of the modern science called nanotechnology [1]. Nanotechnology is any technology made on the scale of “nano” which has particular applications in the real world. It includes the production and applications of systems in the range of individual atoms or molecules [1]. Nanomaterials show peculiar and different physical, biological and chemical properties compared to their bulk counterparts due to the small size [2]. They possess special features such as high reactivity, sizes in the range of nanometers (10^{-9} m), and high ratio of surface area to mass [3]. Nanoparticles (NPs) have been efficiently used in chronic disease diagnostics, in pharmaceutical and medical nanoengineering for drug delivery, in clothing and in the food industry in order to limit bacterial growth [3].

Water is one of the most important resources for human beings. With the development of industry, water pollution is becoming more considerable. Fortunately, membrane separation is one of the most efficient methods to remove the contaminations from water, whose properties of porosity, surface charge, hydrophilic/hydrophobic nature etc. play a vital role in filtration. Among them, electrospun three dimension (3D) porous nanofibrous filtering membrane has received considerable attention due to their high porosity, good interconnectivity, and high specific surface area. Nanocomposite polymeric films can incorporate impressive functional characteristics of nanoparticles with the simple synthesis and low cost advantages of polymer.

The aim of the project was synthesizing nanoparticles (Ag and TiO_2) in the form of suspensions, and producing a composite membrane consisting of polymer fibers and nanoparticles by electrospinning process. Polymer nanofibers produced from polymer solutions by electrospinning possess unique properties such as high porosity and high surface area to volume ratio [4]. These novel physical and chemical characteristics lead composite membranes to various potential applications, particularly of the water purification.

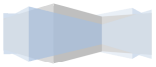

1.1. Silver nanoparticles

In recent years, with the development of a modern medicine, silver became emphasized as an excellent bactericidal agent. It was discovered that silver nitrate kills bacteria and because of that it enhances wound healing [5]. Due to the high reactivity connected with the large surface to volume ratio, silver nanomaterials have an essential role in stopping the bacterial growth. What is more AgNPs possess broad variety of other applications such as excellent optoelectronic properties for diagnosis and imaging. Likewise Silver Nano (Silver Nano Health System) is a trademark name of a bactericidal technology which uses AgNPs in air conditioners, refrigerators, washing machines, vacuum cleaners and air purifiries introduced by Samsung in April 2003. Silver nanoparticles are also used in the interaction with HIV which was demonstrated by Elechiguerra. It is an example of an excellent targeting the surface of certain cell types or specific areas [7].

The bactericidal activity of AgNPs is strictly connected with their size. The smaller the dimension of nanoparticles the stronger the bactericidal effect because the larger the surface area available for interaction [2].

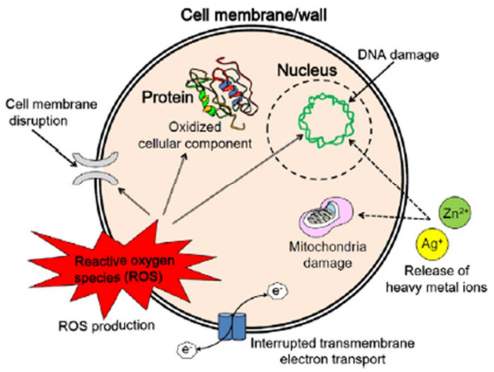

It is crucial to explain the working mechanism of AgNPs to understand their bactericidal effect. The antibacterial properties of silver nanoparticles are connected with their slow oxidation and liberation of Ag^+ ions to the environment which simply means the reduction of Ag ions into elemental Ag in the form of nanoparticles.

Fig. 1 Various antimicrobial mechanisms of nanomaterials [6]

Moreover, the small size of these particles is responsible for easiness in penetration through cell membranes to affect intracellular process from inside. It is responsible for membrane damage and death of the organism [2]. Nanoparticles may also go deeply inside the cell and

interact with phosphorous and sulfur which are present in compounds such as DNA and proteins and may cause damages [7]. Nowadays, the main and most important problems that scientists have to face are developments of multiple drug resistance bacteria due to the use of commercial antimicrobial drugs usually used in the infectious diseases treatment. Commonly used antibiotics are sometimes connected with allergic reactions or may be toxic and irritant [8], that is the reason why silver nanoparticles play an alternative role in the diseases treatment. However, essential property of silver is that in small concentrations it is safe for human cells but lethal for the majority of viruses and bacteria and because of that it is widely used in water disinfection [7]. On the other hand, there is a high concern about the toxicity of AgNPs and probable sub lethal effects on human. The toxic effect of the silver nanoparticles occurs at concentrations of 5 μg mL^{-1} while the antimicrobial activity takes place at concentrations which are much lower, starting from 0,7 μg mL^{-1}. However, it has to be taken into account that the toxicity of silver nanoparticles depends on nanosilver particle size, form, coatings and different experimental design [9].

Silver nanowires (AgNWs), which are one dimension metallic structures, are commonly bigger than silver nanoparticles, that is why they can be observed even by the optical microscope. What is more, they have also lower bactericidal effect, but from the other hand they possess high electrical and thermal conductivities. Thanks to these peculiar properties silver nanowires gained an attention for many applications, such as: photonic crystals, optical polarizers, and surface enhanced Raman scattering (SERS) [1].

1.2. TiO_2 nanoparticles

Since 1970s, with the discovery of titanium dioxide photocatalytical process, the use of it in order to destroy organic compounds from contaminated air or water became of high interest [10]. Nanocrystalline titanium dioxide exists in three polymorphic phases: anatase, brookite and rutile. Anatase is found as small and sharp crystals and its crystalline structure can be prepared in the laboratory by chemical methods, for example by sol-gel method. Among all of the three mentioned crystalline structures, anatase has the highest photocatalytic activity and therefore it possesses an antimicrobial function [3]. This activity is connected with its lattice structure. Each titanium atom is connected to six oxygen atoms in anatase tetragonal unit cell.

The titanium and oxygen atoms are less tightly packed, the octahedron is disorted so its symmetry is lower than orthorhombic as in the case of for instance rutile. Each octahedron is in contact with eight neighbors (four sharing an edge and four sharing a corner). Such a differences in lattice structures result in different mass densities and electronic band structures [11]. Anatase titanium dioxide is commonly used as the semiconductor for dye-sensitized solar cells. The photocatalysis working principle is connected with the light falling on a semiconductor with an appropriate bandgap (or energy difference between the conduction and the valence bands). It creates positive and negative charge carriers represented by holes in the case of positive charge and electrons in the case of negative charge carriers. They can be used to initiate reduction (electrons) and oxidation (holes) reactions at the catalytic surface.

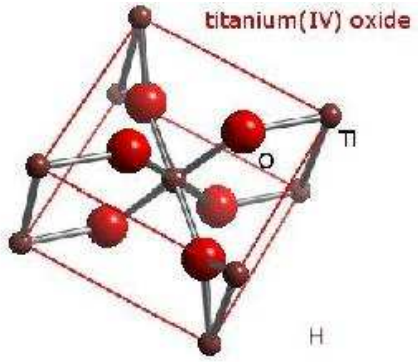

Fig. 2. The crystalline structure of titanium dioxide anatase [12]

However, positively charged holes and negatively charged electrons have a tendency to recombine in order to achieve neutral state, through reemission of a photon (light) or a phonon (heat). Nanoparticles provide the optimal balance between these two effects and due to this fact they are the best for photocatalysis [11].

Lately, TiO_2 photocatalysts have gained an attention as materials used in the cleaning of the environment. Illuminated TiO_2 photocatalysts breakdown organic compounds thanks to oxidation, with holes (h^+) created in the valence band and with hydroxyl radicals ($OH^{\cdot}$) produced by the water oxidation. This particular photocatalytic oxidation produces damage of microorganisms, which consists of organic compounds as well [13]. Nevertheless, there are some doubts about real bactericidal agents. During the photocatalytic reaction there are several other active oxygen species than $OH^{\cdot}$ generated, e.g. hydrogen peroxide (H_2O_2), superoxide anion (O_2^-) and perhydroxyl radical ($HOO^{\cdot}$). Even if hydroxyl radical is considered to be the primary agent in the photocatalytic bactericidal effect, the recent

experiments prove that hydrogen peroxide is the main antibacterial agent due to the fact that it is produced at reduction and oxidation sites of the photocatalysis [13].

1.3. Nanoparticles synthesis-literature review

Silver nanoparticles might be produced using variety of methods: laser ablation, electrochemical method, thermal decomposition, microwave irradiation and sono-chemical synthesis. Chemical and physical methods produce pure and well-defined nanoparticles, however it is important to take into account safety and ecology during the preparation [2]. One of the example of a method producing NPs in an eco-friendly manner is to develop a green synthesis using biological organisms such as microorganisms, plant extract or biomass [2]. Among all of these methods, laser ablation and chemical reduction are the most commonly employed synthetic examples. Metal nanoparticles exhibit a surface Plasmon resonance absorption band in the region of UV-VIS (Ultraviolet visible spectra). The free electrons give rise to the surface plasma band in the conduction band due to the small nanoparticles size. The displace of these bands give a reference on the chemical surrounding, particle size, adsorbed species and dielectric constant [14]. In the chemical reduction methods the silver nanoparticles exhibit a yellowish-brown colour in liquid solution due to the excitation of surface plasmon vibrations. The formation of AgNPs is due to hydrophilic-hydrophobic interactions resulting in the intermolecular force. In this method, there is reduction of metal salt like silver nitrate in an appropriate medium using reducing agents like citrate, borohydride etc [7]. This method was the chosen one in the project due to the low cost, ease of fabrication and low time consumption. The method required some experience so many trials had to be done before obtained results were adequate and satisfactory.

However, apart from experience required, this *"ex-situ"* method does not ensure the monodispersity over a large scale. In the *"in situ"* approach, the nanoparticles are generated in the polymer matrices that possess better dispersion characteristic. In situ fabrication gained lots of interests not only due to the good dispersion ability but also due to the connection between organic and inorganic systems which leads to the new, unique properties. The method ensures also better polymer-particles interaction and it reduces the time of membrane fabrication because it is only a one step process. In this one step approach the metal with zero

charge (M^0) is generated either by the direct reduction of the metal source, salt or another complex, or by the reduction of metal ions by generated intermediates, such as radicals [15]. This method was used in the electrospun membrane fabrication due to the overcoming of the common problems connected with agglomeration of AgNPs, high viscosity of PMMA which made it difficult to disperse NPs in the uniform way. In the following experiment metal nanoparticles were reduced inside the polymer matrix. N,N-dimethyl formamide (DMF) was chosen as a reducing agent. The polymerization of MMA monomers and reduction of silver ions occurred simultaneously which lead to the formation of Ag/PMMA nanocomposites [16].

TiO_2 might be synthesized by variety of different methods such as: chloride process, sulfate process, coprecipitation, impregnation, hydrothermal method, sol-gel method etc. Sol-gel method became one of the most suitable way for synthesizing variety of different metal oxides due to the low processing temperatures, low cost and ease of fabrication. This process involves the transformation from a liquid state “sol” into a solid phase “gel”. The homogeneity of the solid phase depends on a couple of factors such as: the solubility of reagents in the solvent, the temperature, pH and the sequence of addition of reactants [11]. In the case of anatase titanium dioxide photocatalytic process, which was described in the previous sections, switching to more ecological friendly and sustainable methods and technologies, became of high importance in recent years. However, the main limitation of this photocatalyst is that under the visible light condition it does no longer have photocatalytic activity [17]. In order to avoid this problem the solution might be doping titanium by Nd (Neodymium) or other element with absorption in the visible range. Materials of Nd-doped titania which are prepared by mild microwave-assisted protocol possess excellent activities in the photodegradation of water impurity [17].

1.4. Bacteria

The main application of the fabricated membrane will be purifying fresh or drinking water from bacteria, mainly *Staphylococcus aureus* and *Escherichia coli*. Bacteria are a large group of prokaryotic microorganisms, usually with few micrometers length. The main bacteria division is connected with retaining the crystal violet dye in the Gram staining protocol. Gram positive bacteria retain crystal violet dye while the Gram negative do not [18]. *Staphylococcus*

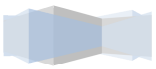

aureus is the example of Gram positive bacteria and might be found in the soil and other environmental areas and can simply contaminate the wound. It can also be taken into account that *S. aureus* in drinking water may be a source for colonizing residents exposed to contaminated water [19]. While the *Escherichia coli* is the example of Gram negative bacteria and can be found in the gastrointestinal system of the human body [10]. There are many sources of *E. coli* contamination, mainly intestinal tracts of human and other warm-blooded animals such as livestock and wildlife. If the concentration of bacteria in a fresh water is higher than the standard numbers there is a high risk of being affected with diarrhea, fewer, chest pain or hepatitis. According to USEPA (United States Environmental Protection Agency) recommendations, some set of agreements connected with the *E. coli* CFU must be obeyed in the fresh water reservoirs [20].

	Designated swimming	**Moderate swimming area**	**Light swimming area**	**Infrequent swimming area**
***E. coli* (CFU/100mL of water)**	235	298	410	576

Table. 1 CFU/100mL of water USEPA recommendations for *E. coli* [20]

E. coli is a major drinking water indicator proving that water is contaminated by for example human or animal wastes. According to European Union's drinking water standards with the Council Directive 98/83/EC on the quality of water intended for human consumption the amount of *E. coli* in the 250 mL of water should be equal to 0 [21].

Antibacterial effect of water filtering membranes against Gram negative and Gram positive bacteria became of high importance. In order to prove the bactericidal properties of nanoparticles, various bactericidal tests might be taken into account. The most popular method for determination the antibacterial activity of various suspensions is agar well diffusion method. The zone of inhibition is examined, which should appear as a clear area around the wells [2]. It was reported that the greater the zone of inhibition the greater the bactericidal effect of the suspension. Moreover, silver nanoparticles have higher influence on Gram-negative than on Gram-positive bacteria. During the treatment by silver ions, DNA loses its replication ability, expression of ribosomal subunit proteins and some other cellular

proteins and enzymes which are crucial to the production of ATP (Adenosine triphosphate) [2]. The inhibition of bacterial growth is dependent on the concentration of AgNPs in the medium [2]. Generally, larger zones are connected with the smaller Minimum Inhibitory concentration (MIC) of antibiotic for that bacterium. MIC is the lowest concentration of an antimicrobial that will stop the growth of bacteria which is visible for a naked eye after 24 hours incubation [18]. Another important bacteria test parameter is Colony-forming unit (CFU) which is an estimate number of viable bacteria or fungi. The units of this number are CFU/ml (colony-forming units per milliliter) or CFU/g (colony forming units per gram) in the case of solids [18].

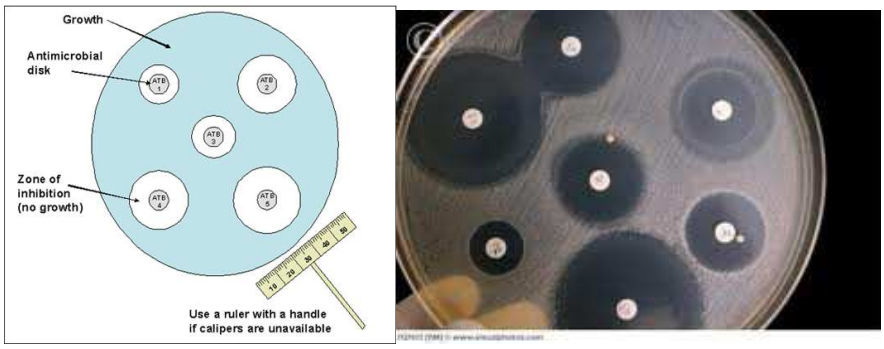

Fig. 3 Agar well diffusion method [22-23]

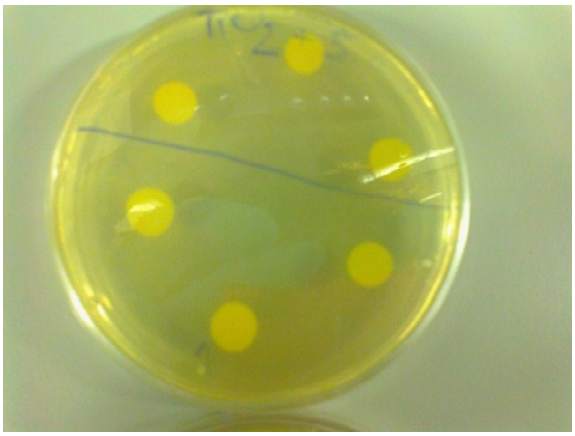

Fig. 4. Dilution bacteria test method

However, more important, accurate and reliable method is dilution bacteria test. The procedure consists of cultivating the bacteria and keeping them in the oven for 24 hours and next, serial dilutions of the suspension starting from 10^8 CFU/ml are prepared. The last step is transferring the solution into Petri plates filled with Agar solution and incubating for 24 hours in the oven once more. The results are examined by visual counting the grown of colony on a Petri plate [24].

1.5. Commercial membranes comparison

Nowadays, population explosion and industrial activities became responsible for large water resources consumption and water pollution. As a consequence, one of the most serious problem and issue is to sustain water balance, in terms of quantity and quality. Membrane technology is recently regarded as essential since it ensures plenty of high grade water with low cost and the maintenance of sustainable water resources [25]. The figure below presents advantages and disadvantages of different membranes according to the material they are made of. Table 3 presents major membrane module designs. It is clearly visible that some characteristic features of membrane, like cost, resistance to fouling, packing density etc., highly depends on the membrane module.

In the designed test the experimentally obtained electrospun membranes were compared to the commercial cellulose acetate membranes in terms of and mechanical resistance.

Figure 3: Pros and Cons of Different Membranes	
CA	
	good permeability and rejection characteristics
	susceptible to hydrolysis
	limited pH resistance
	chlorine tolerant and fouling resistant
PES, PVDF (PS, PAN)	
	ability to modify properties through polymer blend
	good strength and permeability
	PVDF best for flexibility, and use with air scour
	PES best for polymer blending and UF rating
PE, PP	
	susceptible to oxidation
	limited blend capability

Table 2. Advantages and disadvantages of different membranes. (Where, CA: cellulose acetate membrane, PES: polyethersulfone membrane, PVDF: polyvinylidene fluoride membrane, PE: phosphatidylethanolamine membrane and PP: polypropylene membrane.) [25]

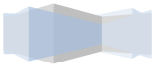

Table 2. Comparing Four Membrane Processes				
	Reverse Osmosis	Nanofiltration	Ultrafiltration	Micro filtration
Membrane	Asymmetrical	Asymmetrical	Asymmetrical	Symmetrical Asymmetrical
Thickness Thin film	150 μm 1 μm	150 μm 1 μm	150 - 250 μm 1 μm	10-150 μm
Pore size	<0.002 μm	<0.002 μm	0.2 - 0.02 μm	4 - 0.02 μm
Rejection of	HMWC, LMWC sodium chloride glucose amino acids	HMWC mono-, di- and oligosaccharides polyvalent neg. ions,	Macro molecules, proteins, polysaccharides vira	Particles, clay bacteria
Membrane material(s)	CA Thin film	CA Thin film	Ceramic PSO, PVDF, CA Thin film	Ceramic PP, PSO, PVDF
Membrane Module	Tubular, spiral wound, plate-and-frame	Tubular, spiral wound, plate-and-frame	Tubular, hollow fiber, spiral wound, plate-and-frame	Tubular, hollow fiber
Operating pressure	15-150 bar	5-35 bar	1-10 bar	<2 bar

Table 3. General comparison of different membrane processes [26]

1.5.1. Cellulose acetate membrane

Among polymer membranes which can be used for separation, cellulose acetate (CA) was one of the foremost. CA, as hydrophilic membrane, possesses a good fouling resistance, its price is low, it has moderate chlorine resistance and good biocompatibility, but at the same time its disadvantages are: poor mechanical strength, low oxidation, thermal and chemical resistances.

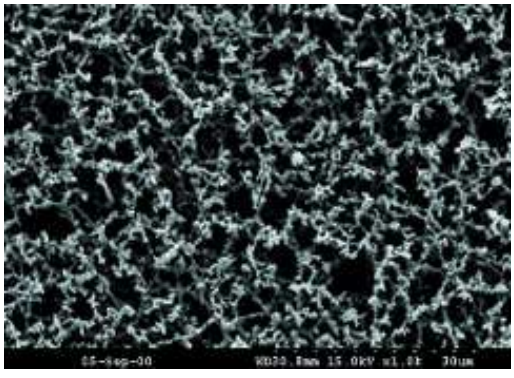

Another obstacle of using CA membranes is crucial for applications in chemical and pharmaceutical industries when organic solvents are part of the feed or in process operating at temperatures higher than 50^{o}C and pH lower than 3 or higher than 7 [27]. Figure 5 presents CA membrane of type ST 68.

Fig. 5.Cellulose Acetate Membrane (Type ST 68, 0.8 μm) [27]

Two commercial filters were examined:

- Cellulose acetate filter by CHMLAB GROUP

These filters with 150 nm diameter possess excellent properties for quantitative and qualitative analysis. They are free of possible residual acids which might be used in some production methods. What is more, they contain extremely low amount of ash [28]

- Cellulose acetate filter by Prat Dumas, France

Prat Dumas filters with the diameter of 0,2 µm, possess an extremely high thermal stability. For this reason they can be autoclaved which is a great property in the bacteria environment. Perfect for biological and clinical analysis [29]

Fig. 6. CHMLAB GROUP and Prat Dumas cellulose acetate filter papers [28-29]

1.6. Electrospinning

Electrospinning process is a simple and low cost technology for producing fibers in the range of few microns by using an electrical charge. In this method the sufficiently high voltage must be applied to a droplet of a liquid, an electrostatic repulsion counteracts the surface tension and the droplet is stretched due to the charge process of the body liquid. At a critical point a stream of liquid explode from the surface. It is called Taylor cone [18]. If the molar cohesion of the liquid is high enough, there is no occurrence of a stream breakup and a formation of charged liquid jet is observed [18]. The current flow alteration from Ohmic to convective mode occurs due to the jet drying in flow. The next step is elongation of the jet by whipping process caused by electrostatic repulsion, until the final deposition on the grounded

collector. The elongation and thinning of the fiber is the result of bending instability which leads to the production of uniform fibers with nanometer-scale diameters [18].

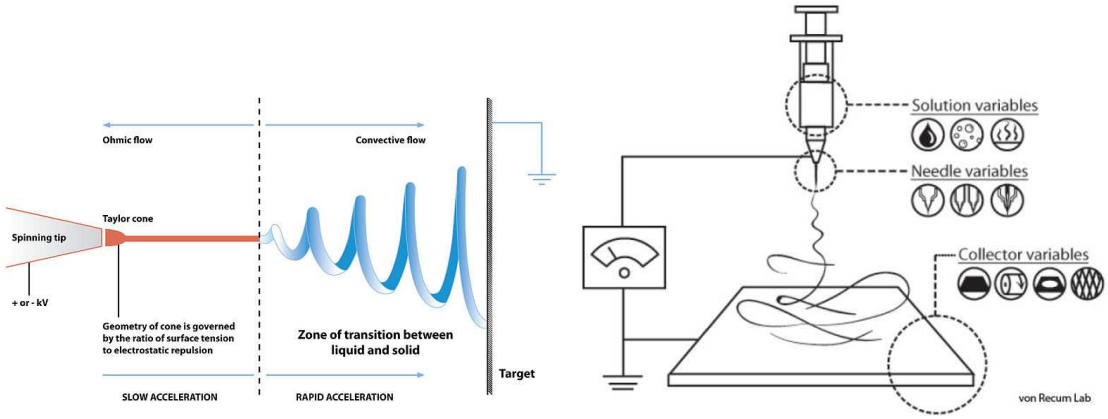

Fig. 7.Diagram showing fibre formation by electrospinning [18].Fig. 8. Electrospinning/electrospraying schematic with variations for different processing outcomes [18].

The typical laboratory electrospinning apparatus consists of a spinneret, which is typically a hypodermic syringe needle, connected to a high voltage (5-50kV), syringe pump, direct current power supply and a grounded collector. A solution is placed in the syringe and the liquid is extruded from the needle tip by a syringe pump at a constant rate. The electrospun non-woven mats provide extremely high porosity and surface area-to-volume ratio. They are light and mechanically flexible which emphasizes their attractive properties for potential applications, for example in biomedical engineering or as filter membranes. Electrospun mats could exhibit higher bactericidal effect than conventional microfibers due to their high surface area-to-volume ratio mentioned above [4].

2. Experimental section

The experimental measurements were taken in laboratories of the Institute of Nanoscience, Aragon (INA) and in the Centro de Investigacion Biomedica de Aragon (CIBA) in Zaragoza, Spain. The first part of the project was synthesizing and characterizing silver and titanium dioxide nanoparticles, testing the bactericidal effect of the suspensions and afterwards the composite membranes were fabricated by electrospinning process made of

Poly(methyl methacrylate) and already synthesized nanoparticles. The last step was verifying the bactericidal effect of created membranes and compare their mechanical resistance with commercial membrane filters for the water treatment.

2.1. Nanoparticles synthesis

Three synthesizing methods were used to produce three different nanoparticles: silver nanowires, silver nanospheres and titanium oxide. Most of the chemicals were purchased from Sigma-Aldrich Co. Spruce Street, St. Louis, USA and PRS Panreac Quimica Sau, Castellar del Valles, Barcelona, Spain.

2.1.1. Silver nanowires (AgNWs) synthesis

Silver nanowires have been used in a broad variety of applications such as: photonic crystals, optical polarizers, microelectronics, catalysts and SERS (Surface Enhanced Raman Scattering). Particularly, great effort was made to obtain nanowires with controllable size [30]. The solvothermal method, developed by the NFP (Nanoporous films and particles) group [30] was used for fabrication of silver nanowires by reducing silver nitrate ($AgNO_3$, 99.9%),with ethylene glycol (EG, 99.8%), and using Polyvinyl pyrrolidone (PVP, molecular weight = 55000), as an adsorption agent with all of the chemicals purchased from Sigma Aldrich.

Two solutions have been prepared in 50 ml beakers:

1. 10 mL of EG and 169,87 mg of $AgNO_3$ (0,1 M)

2. 10 mL of EG and 166,71 mg of PVP (0,15 M)

The first solution was mixed using a magnetic stirrer and the second was added slowly to the first one drop by drop. The second solution was added only after the first one was mixed correctly. The final mixture was placed in the autoclave and closed in the oven for 2,5h in 160^{o}C. Afterwards, the suspension was divided into two plastic centrifugation tubes and thoroughly washed with acetone (10 mL of a suspension and 30 mL of acetone). Tubes were placed in the centrifugation machine (Jouan B4 number 1995/3777a) at 3000 rpm (revolutions

per minute) for 20 min. The procedure was repeated 3 times. After each centrifugation supernatant was removed and replaced again by acetone [31]. The solutions were placed in the ultrasonic bath for about 5 minutes in order to avoid agglomeration of particles after each centrifugation during all of the nanoparticles synthesis.

2.1.2. Silver nanoparticles (AgNPs) synthesis

The synthesis of silver nanospheres was carried out also by a polyol method. It is commonly used for preparation of metals which are easily reducible. The polyols, such as: diethylene or ethylene glycol are able to act as a reducing agent but also as a solvent in which the metal salts might be dissolved or suspended. The capping agents are used to protect nanoparticles from sintering with each other and from forming large particles. PVP is one of the commonly used capping agent [6]. Most of the chemical reducing reactions require elevated temperatures to increase the reaction rate. The energy which is used to heat up the media can be laser irradiation, conventional thermal heating, ultrasonic, UV irradiation etc.

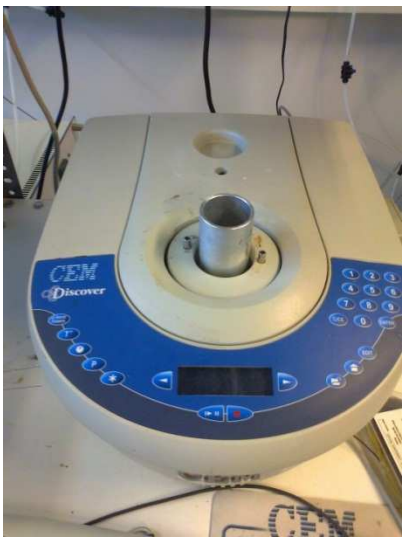

Microwave radiation however, has the fastest heating rate and is used to synthesize platinum and silver nanoparticles. It heats up the material through its dielectric loss, and then it converts the radiation energy into a thermal one [6]. The method used for preparation of silver nanospheres was chemical reduction of silver salt in the presence of a stabilizing agent and MW heating [32].

Fig. 9 Microwave apparatus, CEM Discover, Institute of Nanomaterials Aragon, Zaragoza, Spain

2,4 g of PVP (Mw = 10000) was added slowly to 20 mL of EG and mixed by magnetic stirrer for 2h in the 50 mL beaker. The consecutive step was adding 0,158 g of $AgNO_3$ and mixing for exactly 20 min. The chemicals in this synthesis were purchased from Sigma Aldrich. The solution was placed in the microwave (CEM Discover) for 16 sec in 200^{o}C with

SintNPsAg16s program which produces the smallest nanoparticles in terms of diameter. After cooling the solution down, the tube with the suspension was placed in the centrifugation machine (Beckman Coulter Allegra 64R) for 1h and with the speed of 21000 rpm. The same procedure was repeated 6 times, each time supernatant was taken out only from the top and then filled with water due to the slow precipitation of silver nanospheres [33].

2.1.2.1. In situ silver nanoparticles synthesis

Due to the difficulties connected with obtaining high concentration of AgNPs another synthesis method was applied. In order to fabricate a silver nanoparticles – polymeric membrane by electrospin a particular concentration was required due to the limitations connected with the size of the syringe used by the device. Taking these limitations into account and after many attempts with the solution of silver nanoparticles and different solvents, it was decided that in the case of AgNPs, *"in situ"* synthesis will be applied. As it was described above, *in situ* method possess only one step. Silver nitrate (Sigma Aldrich) was added directly to the polymer solution of Poly (methyl) methacrylate and its solvents and mixed for around 12 hours. DMF as one of the PMMA's solvent worked as a reducing agent. The amount of $AgNO_3$ added was calculated and it was taken into account that the amount of pure silver in the silver nitrate mixture is lower than in the AgNPs solution. What is more, 2%wt of silver was chosen to be in the solution due to its best solubility.

2.1.3. Titanium dioxide (TiO_2) nanoparticles synthesis

TiO_2 nanoparticles were synthesized by a sol-gel method. 2 mL of Titanium Isopropoxide (TIPO - Sigma Aldrich, 97%) was added drop-wise to 30 mL of absolute ethanol (PRS Panreac) in the 50 mL beaker. The solution was mixed by a magnetic stirrer and 3 ml of acetic acid (HAC – Sigma Aldrich, 99-100%) was added. The following step was addition of 5 ml of deionized water and stirring for 5 min again. The solution was placed in the autoclave that was sealed and heated up in the microwave oven (Milestone – microwave laboratory systems, Ethos Plus, High performance microwave labstation) up to 120^{o}C (measured by IR) for 15 min. The next step was isolation of TiO_2 by centrifugation (10 min at 9000 rpm), thoroughly

washing several times with ethanol. The procedure was repeated three times, each time supernatant was removed and replaced by the new portion of the solvent [32].

2.2. Bacteria test for suspensions

In order to obtain pure viable cultures, bacteria had to be suspended in tryptic soy broth (TSB) purchased from Sharlau Chemie S.A, Barcelona, Spain. Two kinds of bacteria were examined: *S. aureus*, and *E. coli* purchased from American Type Culture Collection (ATCC). One bacteria colony was added to the 100 mL glass bottle with 40 mL of TSB and incubated overnight at 37^{o}C [10]. The next step was the drug treatment. Harvested bacteria in the solution of TSB was added to the tube with the drug suspension with the ratio equal to 1:1 and incubated overnight once more. The control sample without drug was prepared as well. The solution was then suspended in phosphate-buffered saline (PBS) until the turbidity of the solution was no more visible, usually 8 dilutions were required. In order to prepare PBS solution several constituents had to be mixed: Potassium chloride (Panreac), Sodium chloride (EMD Millipore corporation 290 Concord road, Billerica MA 01821, USA), Potassium di-hydrogen phosphate (Panreac), Sodium phosphate dibasic (Sigma Aldrich). The last step was pipetting 25 µl drops of the diluted solution on the Petri plates with Agar solution and incubating overnight at 37^{o}C [24]. Figures 11 and 12 presented below represent the bacteria test for suspensions.

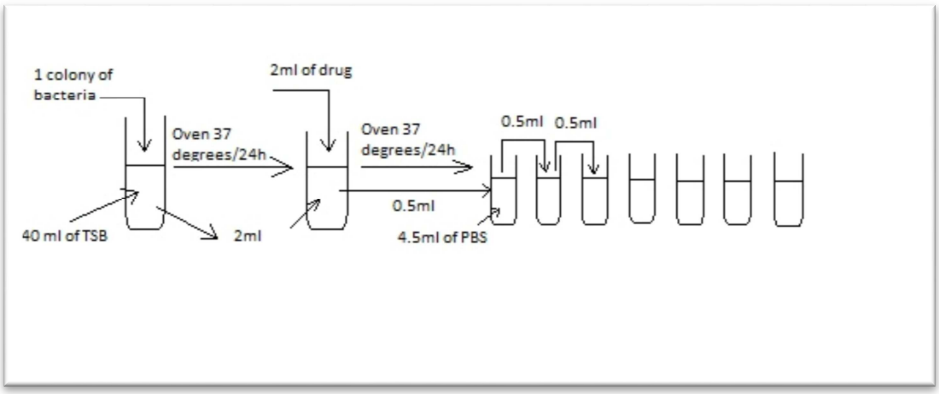

Fig. 10 Representative scheme of the bactericidal test for suspensions

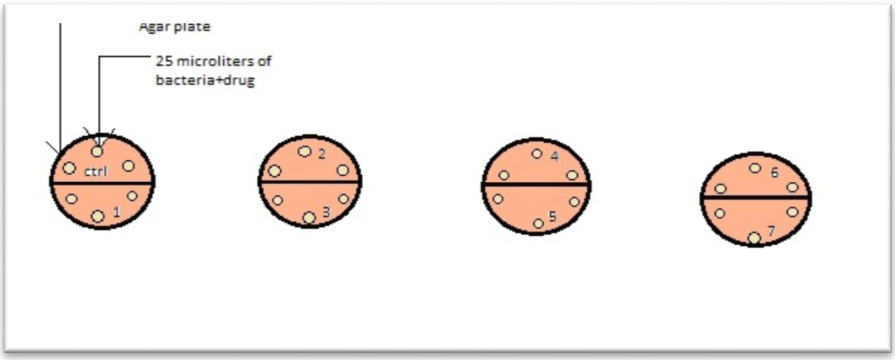

Fig. 11 Representative scheme of the pipetting method for Petri plates

According to the fact that TiO_2 possesses antibacterial activity only under photocatalytic conditions the bacteria test for titanium dioxide was slightly different. A colony of *S. aureus* or *E. coli* were suspended in TSB solution and incubated for 24 h at 37^{o}C. Aliquots of 1 mL aqueous TiO_2 suspension was added to 50 mL glass beaker containing 8 mL of sterilized deionized water and 1 mL of washed bacteria suspension. The samples were placed on a magnetic stirring plate with a continuous mixing and were illuminated with the ultraviolet lamp with and emission equal to 365 nm for 5 h. Finally, the regular dilution method was used in order to verify the bacteria concentration in the irradiated samples [10]. Figures 12-13 present the UV lamp used in the TiO_2 bacteria test procedure.

Fig. 12-13. Ultraviolet lamp VL-4.LC, 365 and 254 nm tubes

All of the nanoparticles suspensions used for a bacteria dilution test must be suspended in water as a solvent in order to be sure that there are nanoparticles which kill bacteria and not the solvent.

2.3. Electrospinning

Flow nanotechnology solutions, Electrospinner 2.2.D-500 was used in order to fabricate the composite membranes. The first objective was to prepare a proper electrospinning solution with good viscosity to avoid droplets from the tip. Figures 14-15 show the electrospinner setup used in INA. The polymer used in the fabrication process was Poly(methyl methacrylate) (PMMA – Sigma Aldrich, Mw = 12000) due to its lightness, low cost and easy handling and processing.

Fig. 14-15 Flow nanotechnology solutions, Electrospinner 2.2.D-500, INA, Zaragoza, Spain

PMMA is a strong material with the density of 1,17-1,20 g/cm^3. It ignites at 460^{o}C and burns, forming CO_2, H_2O, CO and low- molecular-weight compounds (such as formaldehyde) [17]. PMMA is a hydrophobic polymer, which means that the composite membrane most probably will be hydrophobic as well. Poly (methyl methacrylate) possesses environmental stability however, it swells and dissolves in many organic solvents. It is known that the best solvents of PMMA are acetone and N,N-Dimethylformamide (DMF – Sigma Aldrich, Reagent Plus = 99%) [6]. DMF is an organic compound and colourless liquid miscible with water and many other organic liquids. It is a common solvent for chemical reactions [18].

2.3.1. Control sample preparation

The first attempt of PMMA membrane without any nanoparticles was prepared as a control sample. Many attempts of different solutions were prepared, with the best ones

presented below. Each type of membrane was prepared at least twice in order to prove the reproducibility of the process. Acetone and DMF were used as a mixture of solvents in the ratio of 60 to 40 respectively [34]. Different attempts were prepared however, concentrations lower than 18%wt of PMMA did not function due to low viscosity and formation of the liquid droplets on the grounded collector. Two proper samples in terms of viscosity and no droplets formation were prepared with the following concentrations:

- 18%wt of PMMA
- 20%wt of PMMA

While the 20%wt of PMMA was the most stable one. The mass of a polymer which had to be added in order to obtain the desired concentration was calculated from the following formulas:

$$C = \frac{m_{PMMA}}{m_{PMMA} + m_{solvent}}$$

$$C \cdot m_{PMMA} + m_{solvent} = m_{PMMA}$$

$$m_{PMMA} \cdot (1 - C) = m_{solvent}$$

$$m_{PMMA} = \frac{C}{(1 - C)} \cdot m_{sol}$$

$$m = V \cdot \rho$$

$$m = 30mL \cdot 0{,}853 g/mL$$

Where:

C -desired concentration

m-mass [g]

V- volume [ml]

ρ -density [g/mL]

ρ -0,853 g/mL

V -30mL

The same procedure was repeated for different concentrations:

C -20%wt of PMMA

$$m = \frac{0{,}2}{(1 - 0{,}2)} \cdot (0{,}853 \cdot 30)$$

$$m = 6{,}40[g]$$

18%wt of PMMA = 5,623[g]

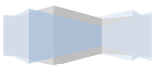

The density of a mixture was calculated from the ratio:

$$\rho_{acetone} = 0{,}791\ g/cm^3$$

$$\rho_{DMF} = 0{,}95\ g/cm_3$$

$$\rho_{mixture} = (0{,}791*0{,}6) + (0{,}95*0{,}4) = 0{,}853\ g/cm^3 = 0{,}853\ g/mL$$

2.3.2. AgNWs/PMMA solution preparation

The calculations presented below shows the volume of AgNWs solution required in order to obtain a proper electrospinning solution, taking into account the concentration of the nanoparticles suspension. The solution had to be well mixed in order to have a well dispersed nanoparticles in the polymer fibers and to avoid agglomeration of particles. Values of two the best solutions are presented below.

First solution calculations:

C - concentration of AgNWs

m - mass of the PMMA

V - volume of AgNWs

C - 4,79mg/mL

m - 6,4 g

30ml of desired solution=18ml of acetone + 12ml of DMF

6,4g of PMMA→1% = 65mg of AgNWs

$$V = \frac{m}{c} = \frac{65mg}{4{,}79mg/ml} = 13{,}57ml$$

18-13,57 = 4,43ml

Substance	Amount
PMMA [g]	**6,4**
AgNWs [ml]	**13,57**
Acetone [ml]	**4,43**
DMF [ml]	**12**

Substance	Amount
PMMA [g]	**6,4**
AgNWs [ml]	**12,9**
Acetone [ml]	**5,1**
DMF [ml]	**12**

Table 4-5. Final amounts of all the constituents of AgNW synthesis

The same procedure was repeated in the second solution with the concentration equal to 5,015 mg/mL.

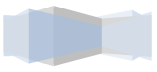

Calculated amounts of constituents were added to a 50 mL beaker and placed on a stirring plate. The constant mixing was kept for about 12 h.

2.3.3. AgNPs/PMMA solution preparation

The silver nanoparticle electrospinning solution was one of the most difficult to prepare. It was connected with the limitation of the concentration value while using electrospinning method. The syringes connected with the rest of the apparatus have only 20 ml volume which means that the solution should have concentration higher than about 4 mg/ml. In the case of silver nanoparticles synthesis obtaining such a high concentration was hard. Many trials was prepared with different solvents, taking into account that there are only two possible solvents: DMF and acetone, to be in agreement with PMMA ones. That is why the *in situ* method was used instead of using a ready solution. However, the results of silver nanoparticles suspensions are presented in the results section as well. The one step *in situ* process required only a direct addition of silver nitrate to the solution of polymer and its solvents. Choosing this technique is possible only in the case of silver nanospheres morphology due to very good distribution characteristic. In the case of silver nanowires the process was not recommended because *in situ* method would not be able to fabricate this particular morphology. Moreover, the size of silver nanospheres fabricated by *in situ* method was very small which will be presented in the characterization section. What is follow that the highest bactericidal effect should be obtained in the *in situ* membrane fabrication due to the smallest size.

Computations were based on the difference in the molecular mass of silver and silver nitrate. $AgNO_3$ was added directly to the solution of polymer instead of AgNPs suspension like it was in the case of AgNWs. Calculations are presented below.

20 mL of solution =12 mL of acetone + 8 mL of DMF

In order to obtain 20%wt of PMMA – 4,269 [g] of PMMA had to be added

In order to obtain 2%wt silver content - 87,12 mg of Ag had to be added

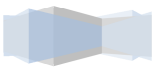

However, $AgNO_3$ is not pure silver which means that some recalculation had to be done:

M_{AgNO3}- 169,87 [g/mol]

M_{Ag} – 107,87 [g/mol]

$m = 87{,}12 \cdot \left(\frac{169{,}87}{107{,}87}\right)$

m = 137 [mg] of $AgNO_3$ had to be added

Substance	Amount
PMMA [g]	**4,269**
$AgNO_3$ [mg]	**137**
Acetone [ml]	**12**
DMF [ml]	**8**

Table 6. Final amounts of all the constituents of AgNPs in situ synthesis

2.3.4. TiO_2/PMMA solution preparation

The last fabricated film was the titanium dioxide membrane. Solution with 7,8 mg/mL concentration was treated in the same way as the previous ones. TiO_2 solution exhibited one of the best dispersion in the polymeric fibers which was visible in the SEM characterization technique. The amounts of all the constituents added to the mixture are presented in table 7.

Substance	Amount
PMMA [g]	**6,4**
TiO_2 [ml]	**8,32**
Acetone [ml]	**9,67**
DMF [ml]	**12**

Table 7. Final amounts of all the constituents of TiO_2 synthesis

2.4. Membrane bacteria test

A bacteria colony had to be suspended in TSB solution and incubated for 24 h at 37°C in order to prepare the bacteria test for solids. 1 ml of the suspended bacteria was transferred to the 1 L Agar solution, which was autoclaved before and which had exactly 37°C. The proper temperature was crucial due to the Agar solution and bacteria properties. Above 37°C bacteria would be killed and below this temperature Agar solution would start to solidify. After stirring the Agar and bacteria mixture, 1 ml of the solution was placed on the membrane by the micropipete, as it is shown in the Figure 16. Small (3cm x 3cm) piece of membrane was placed in a plastic Petri plate which was situated inside the big glass Petri plate filled with

water. The water was required in order to sustain the aqueous environment for bacteria. Petri plates together with the membrane and bacteria were inserted into the oven for 24 h at 37^{o}C. The last step was transferring the membrane into the 50 mL beaker filled with 10 mL of TSB, mixing it and sonicating for 1 min. Then, the standard dilution and bacteria test was prepared [34].

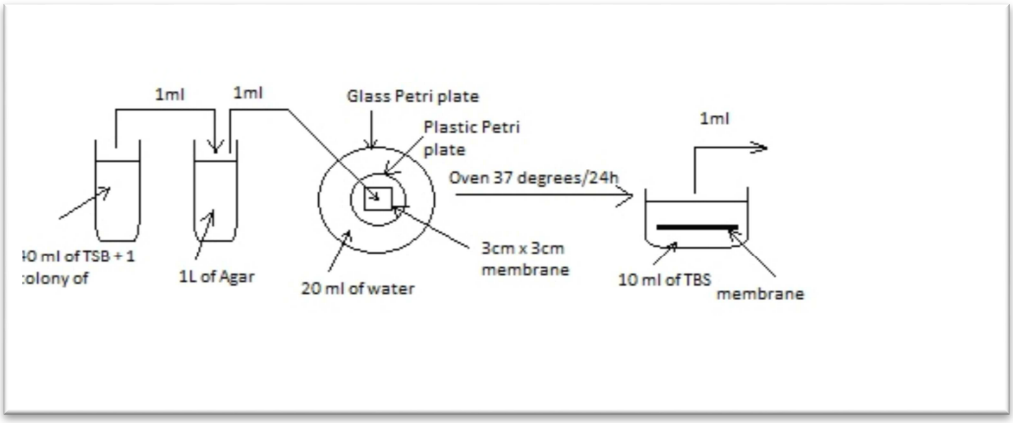

Fig. 16 Representative scheme of the solids bacteria test

In order to prepare titanium dioxide bacteria test for solids different procedure must be taken into account. The different part was connected with the treatment of the Petri plates with the membrane. The membrane was illuminated with the UV lamp for 5 h with 365 nm wavelength at room temperature instead of placing it into the oven. This particular treatment is connected with the TiO_2 different properties under ultraviolet light.

Fig. 17 Titanium dioxide membrane bacteria test under UV illumination

3. Results and discussion

The characterization was divided into two parts: characterization of nanoparticles suspensions and characterization of composite membranes obtained by electrospinning technique. High amount of trials was done in case of nanoparticles suspensions and

electrospun membranes. The best results have been chosen and presented below. What is more, the biggest problem was the choice of a proper solvent because PMMA solvents are acetone and DMF as it was mentioned above. The idea was to use one of these solvents in the nanoparticle synthesis.

3.1. Characterization of nanoparticles

Silver and titanium dioxide nanoparticles were synthesized by methods described in the previous sections. The silver nanowires solution became brownish/grey, silver nanoparticles turned to pale brown and titanium dioxide solution was white.

3.1.1. Microscopy and diameter distribution examination

Microscopy is one of the best technique for characterization of nanoparticles in terms of morphology. Transmission electron Microscopy (FEI TECNAI T20) and Scanning Electron Microscopy (INSPECT S) were used in order to characterize obtained suspensions (TEM) and membranes (SEM).

TEM sample preparation did not required special treatment, diluted suspension was poured on a grid and dried, while in the case of SEM the sample needed to be conductive, hence the drop of a solution was placed on a carbon tape.

What is more, the microscopy examination was combined together with the particle size histograms. The diameter distribution histograms were obtained in the computer software IMAQ Vision Builder from at least 50 measurements of different TEM images. Figures 18-26 represent TEM and SEM (in the case of nanowires) and diameter size distribution histograms images of silver nanowires, silver nanoparticles and titanium dioxide respectively.

Silver nanoparticle suspensions which finally were replaced by *in situ* method in the membrane fabrication are presented in the results below as well in order to prove the reproducibility and to show the working mechanism of the method.

Silver nanowires presented in the figures below show satisfactory particle size distribution. One of the images is a SEM photo which proves that AgNWs are nanoparticles with the biggest size.

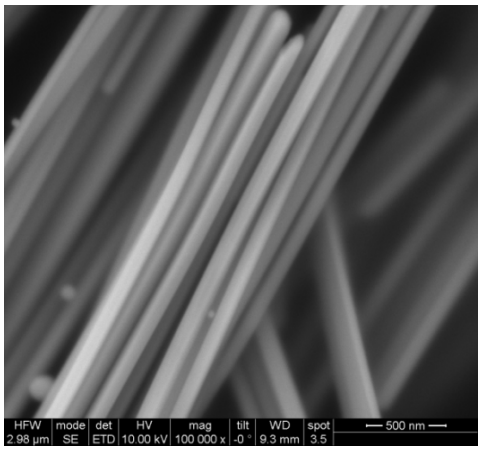

Fig. 18. SEM image of Silver nanowires

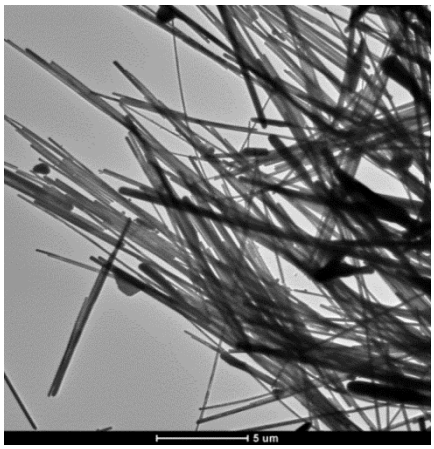

Fig. 19. TEM image of silver nanowires

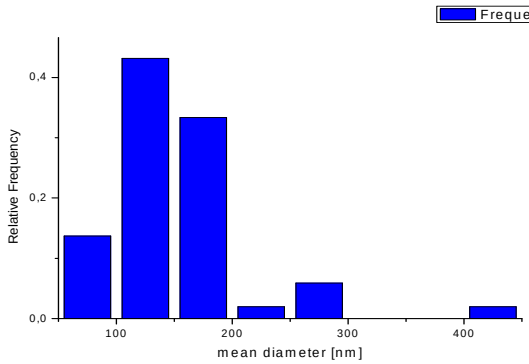

Fig. 20. Particle size distribution of Ag nanowires

The silver nanowires histogram shows that the wire diameter distribution range from 63,3 to 439 nm with the mean diameter equal to 148 nm. It is very difficult to obtain uniform distribution in case of AgNWs due to their agglomeration even after sonication of the suspension used for sample preparation.

Silver nanoparticles presented in the figures below exhibit one of the smallest particles size and better diameter distribution in comparison to the silver nanowires.

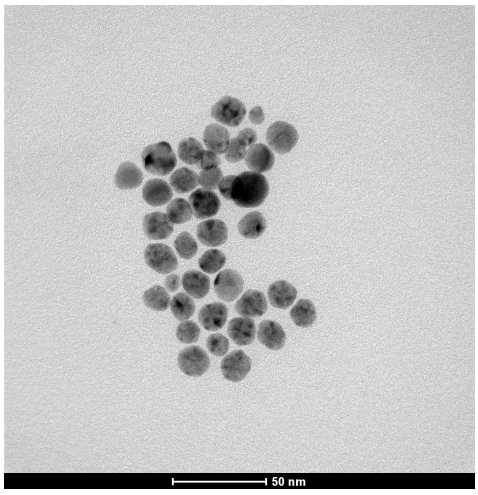

Fig. 21. TEM image of silver nanospheres

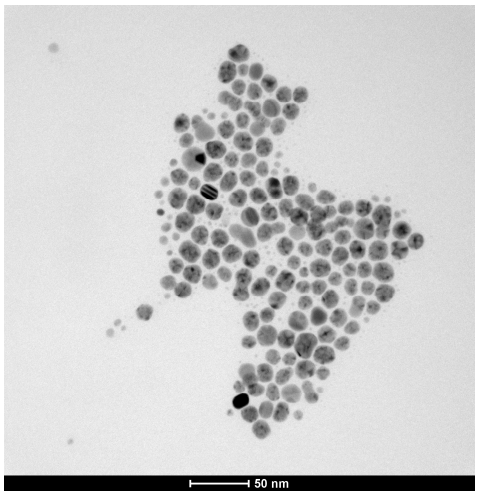

Fig. 22. TEM image of silver nanospheres

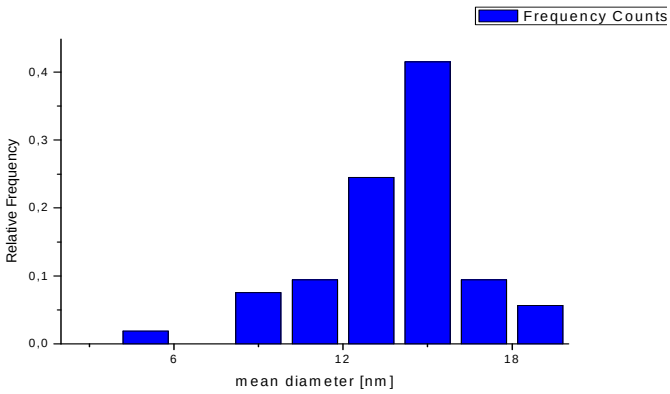

The silver nanoparticles histogram exhibits the mean particles size between 4,06 and 19 nm with the mean diameter equal to 13, 9 nm.

Fig. 23. Particle size distribution of Ag nanoparticles

Titanium dioxide anatase nanoparticles exhibit a tendency of agglomeration, however their particles size distribution is good and the size is also small. Nevertheless, it was a big challenge to keep TiO_2 nanoparticles not agglomerated with each other due to the high concentration of the suspension with acetone which caused the particles agglomerate at the bottom of the sample.

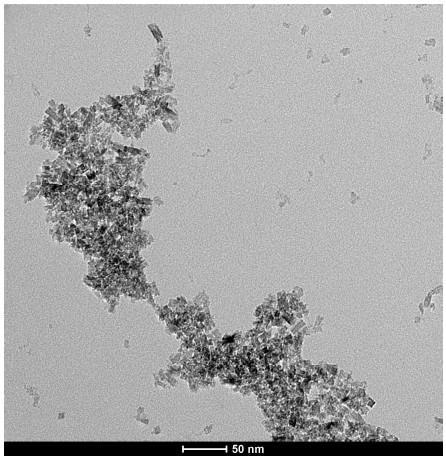

Fig. 24. TEM image of TiO_2

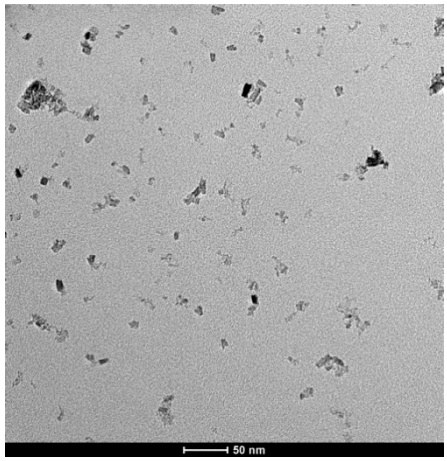

Fig. 25. TEM image of TiO_2

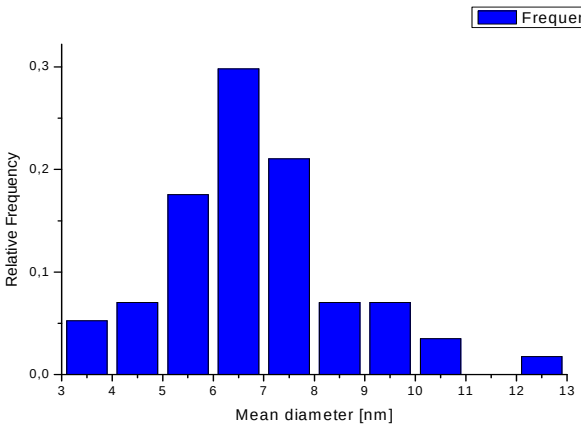

The TiO_2 particle size histogram shows the particles range between 3,56 and 12,4 nm with the mean diameter 6,8 nm.

Fig. 26. Particle size distribution of TiO_2

From the histograms above it is clear that the biggest nanoparticles are silver nanowires and the smallest titanium dioxide nanoparticles.

3.1.2. UV-visible spectroscopy

UV-visible spectroscopy is a commonly used technique for structural characterization of nanoparticles. The measurements were carried out in Jasco V-670 Spectrophotometer in the Institute of Nanoscience of Aragon in Zaragoza, Spain. The range of the measurement was between 800 and 300 nm. Three suspensions were examined: silver nanowires, silver nanoparticles and titanium dioxide respectively. The results are presented in the figures below.

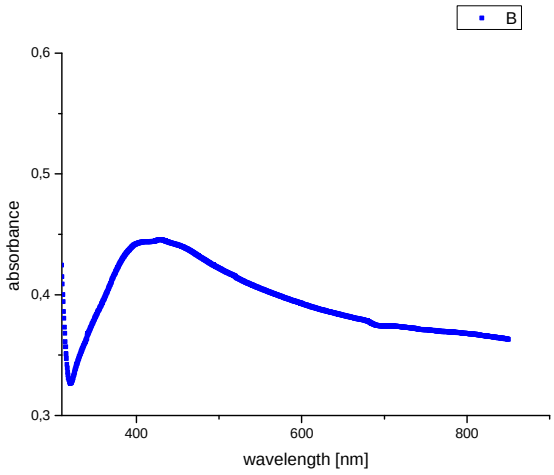

Fig. 27 UV-Vis absorption spectrum of silver nanowires

The absorption spectrum of silver nanowires presented in the Figure 27 shows a surface Plasmon absorption band with the value of 429 nm demonstrating the presence of silver nanowires. The colour of the solution was brownish/grey with a high turbidity which had an influence on the sharpness of the peak [36].

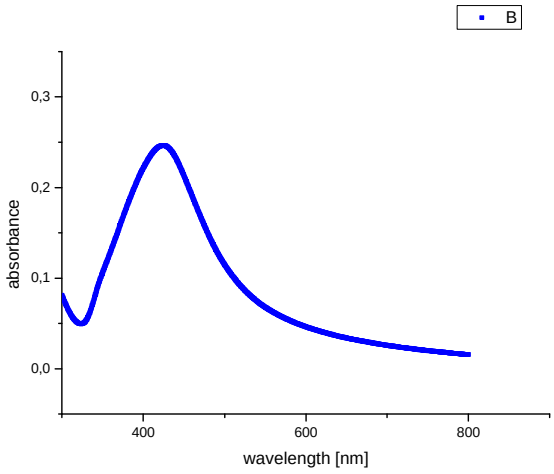

Fig. 28 UV-Vis absorption spectrum of silver nanoparticles

The absorption spectrum of silver nanoparticles presented in the Figure 28 is equal to 424,5 nm and the peak is sharper than in the case of nanowires. It is connected with the pale brown colour and no turbidity present in the solution [36].

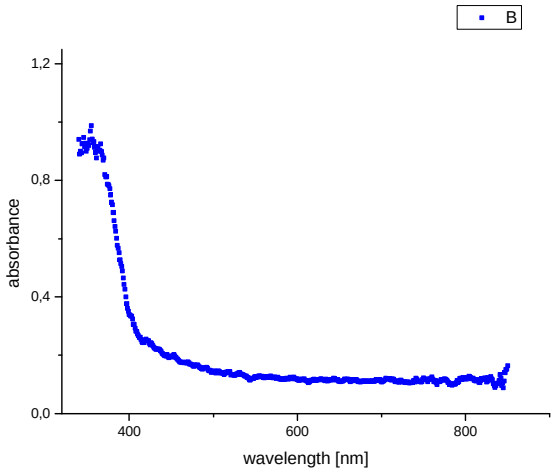

Fig. 29 UV-Vis absorption spectrum of titanium dioxide

The last figure shows the absorption spectrum of TiO_2 nanoparticles in the form of anatase. The surface Plasmon absorption band exhibits its maximum at 363 nm which indicates titanium dioxide particles [37]. What is more, the reason of the peak getting sharper is the decrease of the size of nanoparticles which was indicated by the particle size distribution in the previous section [37].

All of the presented above spectrums indicated the presence of AgNWs, AgNPs and TiO_2 nanoparticles respectively.

3.1.3. Concentration measurement by microbalance

The measurements were carried out using RAWDAG, Wagi Elektroniczne, MYA 5/2Y, Poland microbalance in order to check the concentration of the solutions which was a crucial characterization technique for the usage by electrospinning. The small aluminum vessels were used in order to weight the solution in the microbalance. First, empty vessels were measured, and after they were filled with the solution and placed into the oven in order to evaporate the solvent. The vessels were weighted once more and the difference was used to plot the graph: mass versus volume. The resulting graph was a linear representation of the amount of the nanoparticles in the suspension. The linear function with the formula: $y = ax + b$ demonstrates the values of intersection (y) and the slope (a) of the curve. The value of the concentration is equal to 1/a.

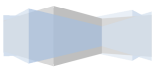

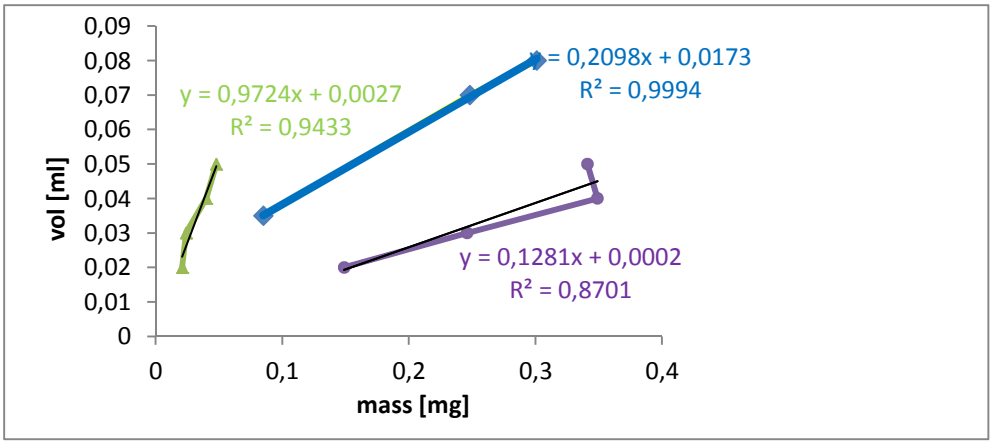

Fig. 30 Linear representation of nanoparticles suspensions used for producing a composite membranes

The graph above represents the silver nanowires (blue colour), silver nanoparticles (purple colour) and titanium dioxide (green colour) linear representations. The values of concentrations are presented in the table below. Many attempts were done in order to check concentrations of many solutions. Only three of them are presented in this section.

Nanoparticles solution	**Concentration [mg/ml]**
AgNWs	4,78
AgNPs	1,02
TiO_2	7,8

Table 8. Concentration values of different nanoparticles

3.1.4. Zeta potential

Zeta potential measurements were important in terms of the stability of the solution. The measurement was taken by PALS- Phase Analysis Light Scattering, which is an extension of laser, Electrophoretic Light Scattering (ELS). ELS is used to the measurement of the velocity of moving particles that scatter laser light, to the measurement of electrophoretic mobility (EPM) and the calculation of zeta potential.

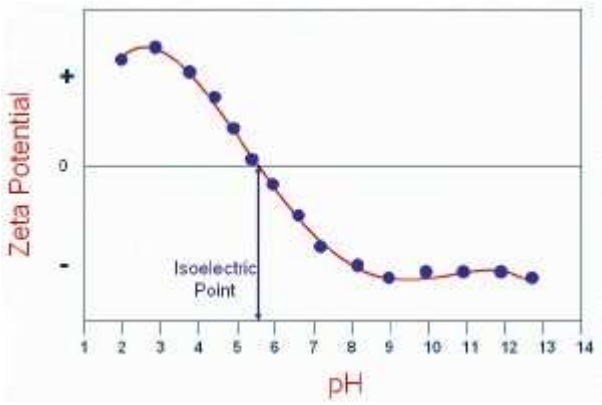

Fig. 31 Zeta potential figure representing values for stable and unstable solutions [38].

According to the literature, solutions with high negative or high positive values of zeta potential are stable, while those with low values, close to zero are not stable. Particles are in the constant movement (Brownian motion), if they exhibit high zeta potential values it means that they have big charges and they repulse from each other, which means no attraction occurs and the solution is stable [18].

Zeta potential measurements of three nanoparticle suspensions indicated their stability at their natural pH. Results are presented below:

NPs	**pH**	**Zeta potential**
AgNW	6,65	-16,51
AgNP	5,94	-14,86
TiO_2	5,17	+21,6

Table 9. Zeta potential values for NPs at their original pH

None of the suspension exhibit value of zeta potential close to zero, which means suspensions are stable because the more negative or positive value of zeta potential the highest the stability. The most stable should be titanium dioxide suspension with the highest zeta potential value. But in the electrospinning process titanium dioxide was added to the acetone suspension where the agglomeration tendency increases.

3.1.5. Raman spectroscopy

Raman spectroscopy technique takes into consideration inelastic scattering (Raman scattering) of monochromatic light which usually comes from laser in the visible or ultraviolet range. The light of the laser interacts with molecular vibrations which results as an energy of the laser photons being shifted up or down. That particular shift is different for different compounds so it gives information about the vibrational modes in the system [18]. Two samples were carried out in order to examine the spectroscopy of the system: suspensions

containing silver and titanium dioxide nanoparticles. The suspensions were dried in order to obtain the pure nanoparticles without the solvent and were placed on the optical microscopy glass.

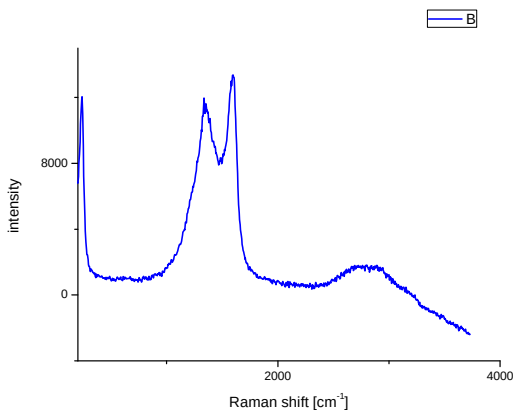

The Raman spectroscopy figure shows variety of bands: 1596 cm^{-1} for glassy carbon [39], 1319cm^{-1} lonsdaleite (hexagonal diamond) [40], 2847 cm^{-1} for CH_2 stretching [41] coming from carbon contamination, while the most important is silver bonding: 245 cm^{-1} for Ag-O [42].

Fig. 32. Raman spectroscopy for AgNPs

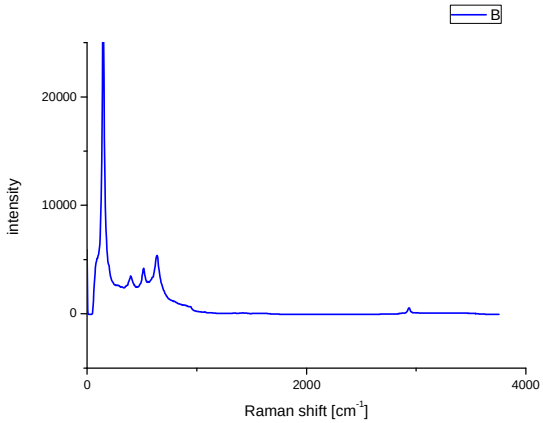

The Raman spectroscopy figure shows the dominating bands of 639, 502 and 406 cm^{-1} which are the typical peaks for titanium dioxide anatase [43-44]

Fig. 33. Raman spectroscopy for TiO_2

3.1.6. Bacteria testing

The bacteria testing measurements were held in CIBA (Centro de Investigacion Biomedica de Aragon). Tests with two kinds of bacteria strains were examined: *S. aureus* and *E. coli*. Two different bacteria testing were carried out: suspension bacteria test and bacteria test for solids in order to test the fabricated electrospun membranes. The results are presented in the figures below.

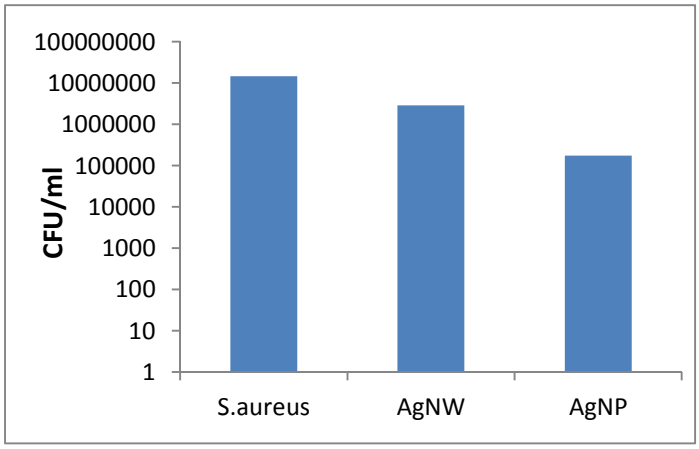

Fig. 34. Bacteria test of AgNWs and AgNPs against *Staphylococcus aureus*

Suspensions of AgNPs and AgNWs with concentrations of 1,03 mg/mL and of 1,13 mg/mL respectively were examined against *S. aureus* bacteria strain. Both concentrations were kept similar in order to compare their results. As it is presented in the Fig. 34. AgNPs exhibit better bactericidal effect due to the small size [2].

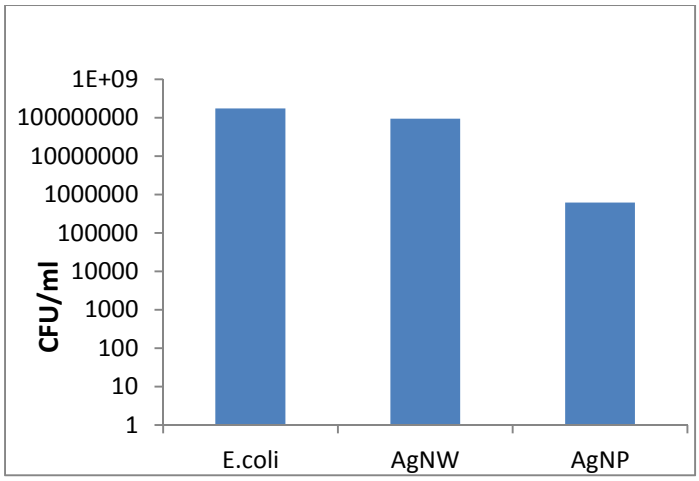

Fig. 35. Bacteria test of AgNWs and AgNPs against *E. coli*

The same solutions were used in order to test the *E.coli* bacteria resistance. As it was mentioned in the previous sections and proved by the Figure 35 silver exhibits stronger bactericidal effect against Gram negative bacteria, where *E.coli* is one of them.

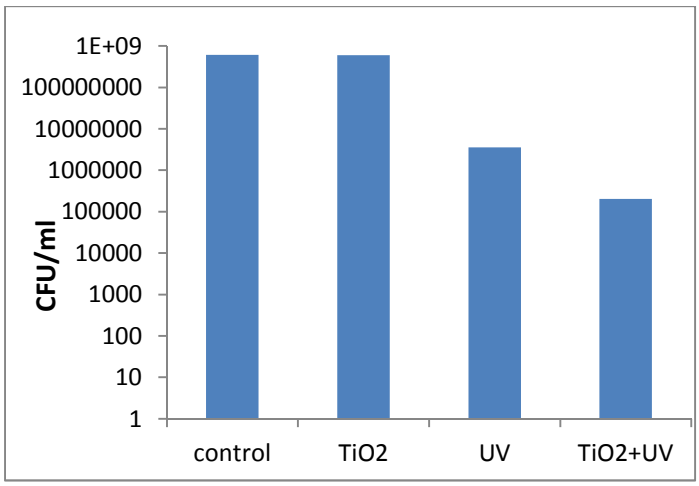

Fig. 36. Bacteria test of titanium dioxide suspension against *S. aureus*

TiO_2 suspension with the concentration equal to 1,5 mg/mL was examined against *S . aureus* bacteria strain. Three samples were measured: TiO_2 illuminated by UV lamp, TiO_2 without illumination and the last sample was just illuminated by UV without TiO_2. It can be seen that the nanoparticles have no bactericidal action without UV irradiation, the radiation itself

presents some bactericidal effect but the combination is the most effective system to reduce the bacteria population.

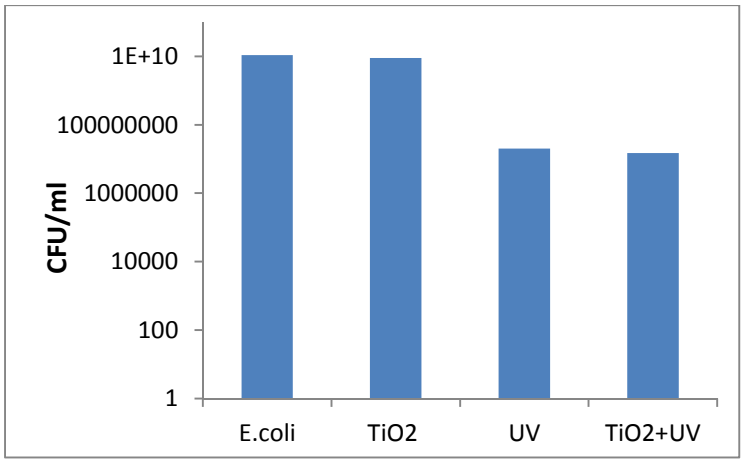

Fig. 37. Bacteria test of titanium dioxide suspension against *E. coli*

Titanium dioxide with the same concentration as described above was examined against *E.coli* bacteria strain. The procedure of three measurements was the same as in the previous attempt. In this case the presence of nanoparticles has little effect in the bactericidal activity. Moreover, TiO_2 did not affect Gram negative bacteria.

Bacteria	Nanoparticles	Value [CFU/ml]
S.aureus	AgNW	$2,84*10^6$
	AgNP	$1,74*10^5$
E.coli	AgNW	$9,33*10^7$
	AgNP	$6,18*10^5$
S.aureus	TiO_2+UV	$2,02*10^5$
E.coli		$1,48*10^7$

Table 10. Colony forming units values of the three suspensions examined against *E.coli* and *S. aureus*

Even though all the particles present bactericidal activity, as it was expected, the smallest silver nanoparticles are the most effective.

3.2. Membrane characterization

Silver nanoparticles, silver nanowires and titanium dioxide membranes were fabricated by the electrospinning method described in the experimental section. Almost the same characterization methods were used as in the case of suspensions with TGA (Thermogravimetry analysis) instead of microbalance and mechanical resistance of a membrane as an additional measurement techniques.

3.2.1. Electrospinning parameters

Fabricating a proper fiber surface by electrospinning required setting up many parameters. The most important are presented in the tables below:

Concentration	18%wt of PMMA	20%wt of PMMA
Distance tip-collector [cm]	15	15
Humidity [%]	39,54	28,05
Temperature [^{o}C]	23,47	22,20
Pump 1 speed [ml/hour]	0,5	0,5
Pump 2 speed [ml/hour]	0,1	0,1
Diameter*	15,9	15,9
Voltage injector [kV]	4,08	3,02
Voltage collector [kV]	-2,41	-2,53
Time [hrs]	5	7

Table 11. Measurement parameters for different concentrations of PMMA fibers;

*pump diameter for 10ml Norm Ject syringe

The parameters in the following measurements were kept constant with the slight changes in time, voltage injector and collector and pump speeds in order to obtain the most uniform and stable flow. Moreover, the pump diameter value changed when the syringe used in the eletrospin device changed as well. For Norm Ject 10 ml syringe the pump diameter was equal to 15,9 while for 10 ml BD syringe the value was 14,5.

3.2.2. Microscopy and diameter distribution examination

Many attempts were done before the best composition was discovered. The change in the diameters of PMMA nanofibers may be the result of different experimental parameters. Variation of temperature or humidity can have an influence and it might be a possible explanation. Likewise with broad values of voltage injector and collector, usually the values are slightly different from solution to solution which is connected with different viscosities. The first task was finding the best and the most stable polymer solution. Next step was adding the nanoparticles solution and fabricating the composite membrane. The figures below

represent the polymer fibers, AgNW + polymer, AgNP + polymer and TiO_2 + polymer respectively.

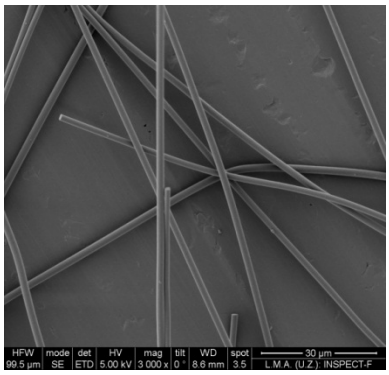

Fig. 38 SEM image of 16%wt PMMA fibers

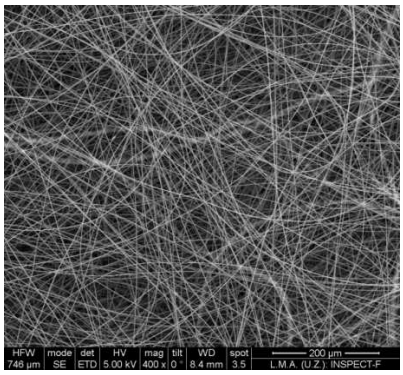

Fig. 39 SEM image of 18%wt PMMA fibers

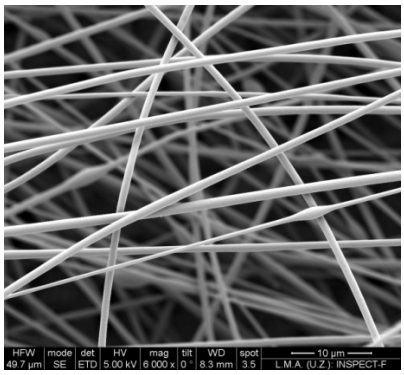

Fig. 40 SEM image of 20%wt PMMA fibers

The 20%wt of PMMA was decided to be the most stable in terms of lack of liquid droplets, good viscosity, and the best membrane texture.

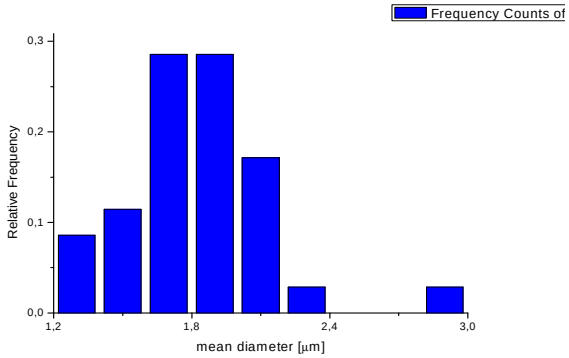

Fig. 41. Fiber size distribution of 16% wt ofPMMA fibers

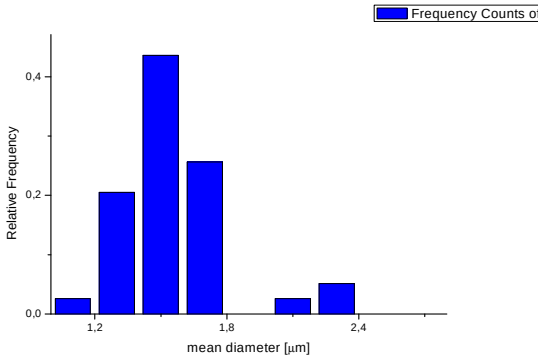

Fig. 42. Fiber size distribution of 18% wt of PMMA fibers

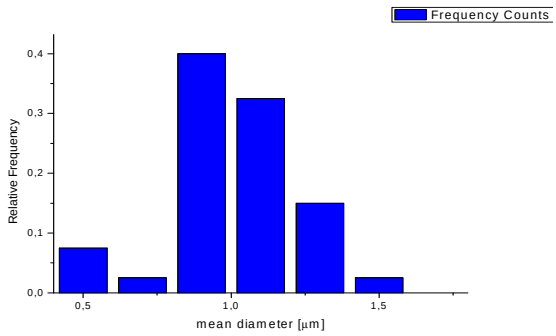

Fig. 43. Fiber size distribution of 20% wt of PMMA fibers

Figures above show histograms with the fiber size distribution of PMMA with 16%wt and the mean diameter of 1,83 µm, PMMA with 18%wt with the mean diameter of 1,56 µm and PMMA with 20%wt and the mean diameter of 0,99 µm respectively. The diameter distribution histograms of polymer fibers indicate the smallest filaments being the one of 20 %wt of PMMA.

What is more, the most uniform diameter distribution is also exhibit by the same fibers.

Final experimental step was fabrication of electrospun composite membranes. Three different membranes were fabricated: AgNWs, AgNPs and TiO_2 respectively. Results are presented below.

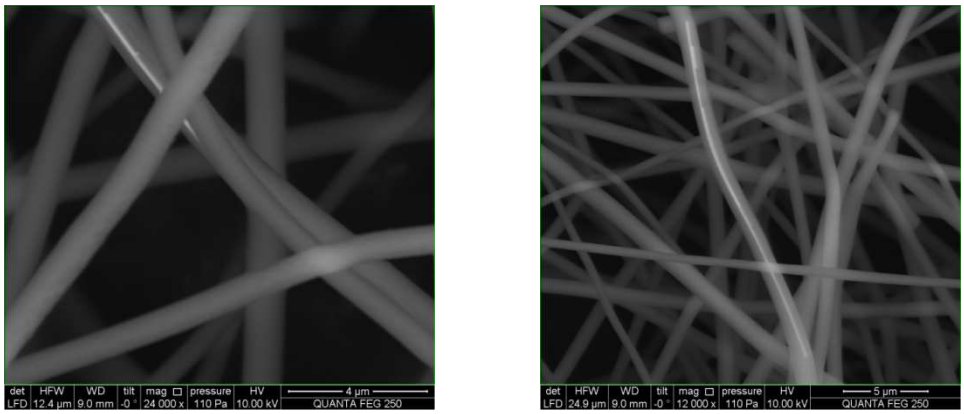

Fig. 44-45 SEM images of silver nanowires incorporated into PMMA fibers

Silver nanowires exhibit lower dispersion characteristic than silver nanoparticles presented below due to bigger size and tendency of agglomeration.

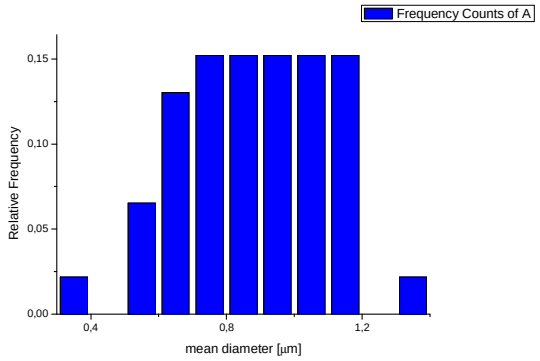

Fig. 46. Fiber size distribution of PMMA fibers with AgNWs

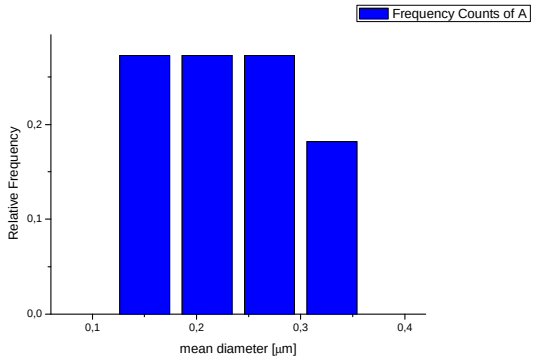

Fig. 47. Particle size distribution of AgNWs incorporated into PMMA fibers

Figures 46-47 show the fiber size distribution histograms of PMMA in the sample of AgNWs+PMMA with the mean diameter equal to 0,88 µm and the particle size distribution of AgNW in the sample of AgNWs+PMMA with the mean diameter equal to 0,22 µm respectively.

Silver nanoparticles membranes fabricated by *in situ* method exhibit the best and the most uniform distribution characteristics. Results are presented in the figures below.

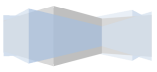

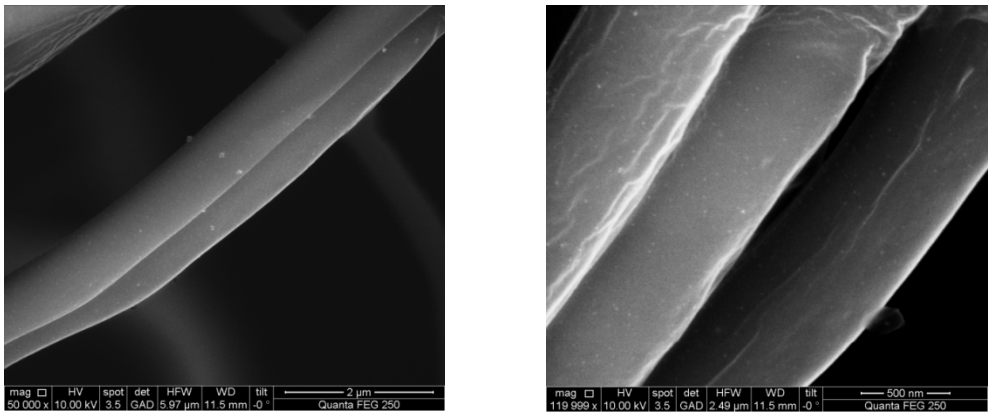

Fig. 48-49 SEM images of silver nanoparticles incorporated into PMMA fibers

Silver nanoparticles incorporated into PMMA fibers and synthesized by *in situ* method exhibit great distribution inside polymer fibers.

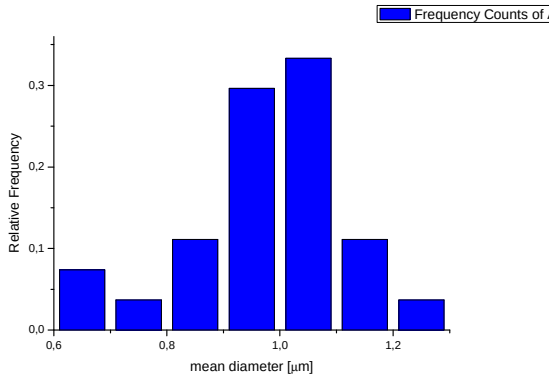

Fig. 50. Fiber size distribution of PMMA fibers with AgNPs

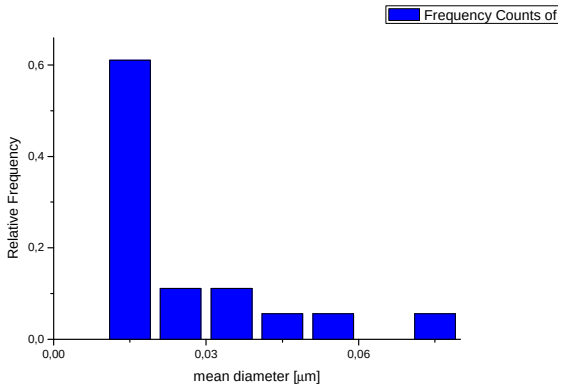

Fig. 51. Particle size distribution of AgNPs incorporated into PMMA fibers

The histograms presented above show the fiber diameter distribution of PMMA in the sample of AgNPs + PMMA with the mean diameter equal to 0,98 µm and the nanoparticle size distribution of AgNPs in the sample of AgNPs + PMMA with the mean particle size equal to 0,023 µm.

The small size and the best distribution of silver nanoparticles are connected with, *in situ* synthesis method a one step process that assures the good distribution of the nanoparticles precursors in the polymeric matrix and avoid the agglomeration find in the suspension produced by the usual synthesis method.

Titanium dioxide membrane presented in the figures below exhibits very good particle distribution as well. TiO_2 tends to agglomerate in the acetone suspension due to the high concentration.

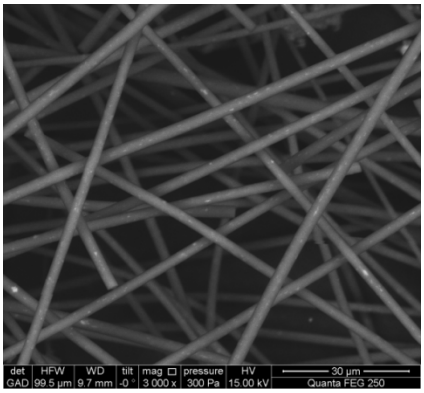

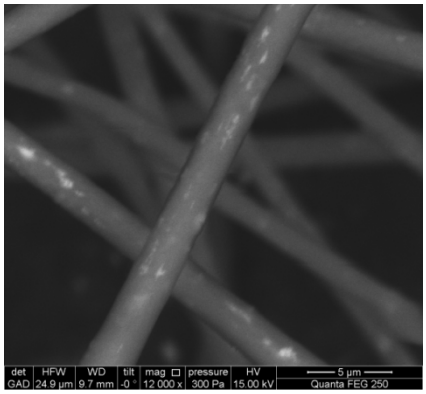

Fig. 52-53 SEM images of titanium dioxide incorporated into PMMA fibers

TiO_2 nanoparticles present good distribution with the most uniform diameter distribution as it is shown in next sections.

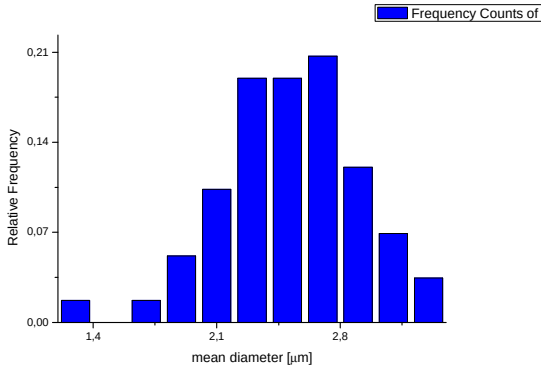

Fig. 54. Fiber size distribution of PMMA fibers with TiO_2

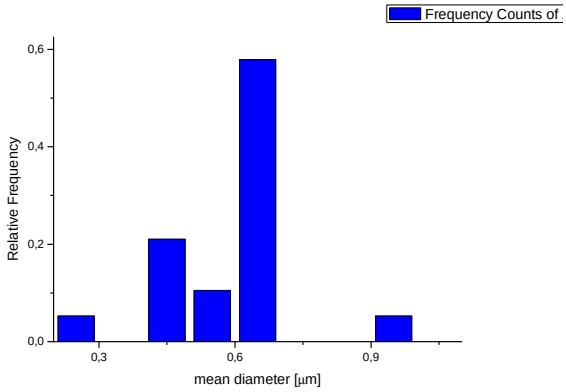

Fig. 55. Particle size distribution of TiO_2 incorporated into PMMA fibers

The histograms show the fiber size distribution of PMMA in the sample of TiO_2 + PMMA with the mean diameter equal to 2,51 µm and the particle size distribution of TiO_2 in the same sample with the mean diameter equal to 0,59 µm showing the agglomeration of the primary nanoparticles.

As it is visible from the results above, the PMMA fibers with the highest diameter are present in the case of TiO_2 + PMMA membrane, and the lowest for AgNW + PMMA membrane. What is more, the most uniform nanoparticles diameter distribution is observed for the AgNP + PMMA *in situ* membrane due to the excellent distribution characteristic of the method which was described in the previous sections.

3.2.3. UV-VIS

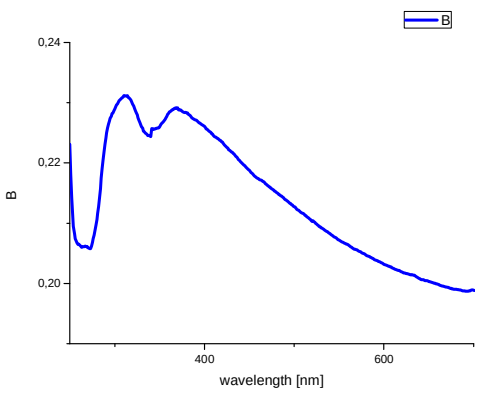

The absorption spectrum of silver nanowires + PMMA membrane presented in the figure shows a surface Plasmon absorption band with the value of 373 nm demonstrating the presence of silver nanowires [36]. Presence of two peaks might be a reason of a non-homogenous silver nanowires distribution.

Fig. 56. UV-Vis absorption spectrum of AgNWs/PMMA membrane

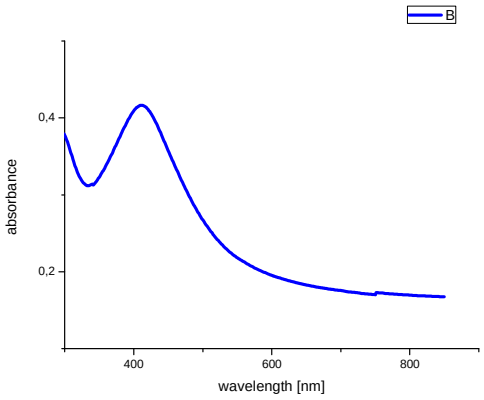

The absorption spectrum of silver nanoparticles + PMMA membrane presented in the figure is equal to 410 nm and the peak is sharper than in the case of nanowires. It is connected with better *in situ* silver nanoparticles distribution inside polymer fibers than in the case of nanowires [36].

Fig. 57. UV-Vis absorption spectrum of AgNPs/PMMA membrane

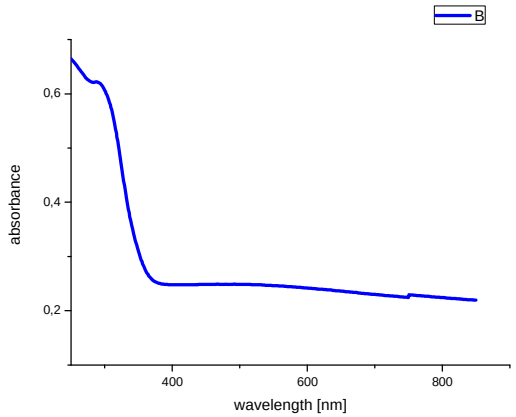

The last figure shows the absorption spectrum of TiO_2 nanoparticles in the form of anatase + PMMA membrane. The surface Plasmon absorption band exhibits its maximum at 288 nm which indicates titanium dioxide nanoparticles [37].

Fig. 58. UV-Vis absorption spectrum of TiO_2/PMMA membrane

3.2.4. TGA

Thermogravimetric analysis is a thermal analysis method where changes of the chemical and physical properties of an examined material are measured as a function of an increasing temperature. TGA can provide information about physical phenomena, for example decomposition [18]. This method was used in order to find out what was the concentration of the nanoparticles inside the polymeric membrane matrix. Proper heating temperature was required in order to decompose the polymer but not the nanoparticles. The process finished when the whole amount of polymer evaporated and after simple calculations the concentration of the nanoparticles could be estimated.

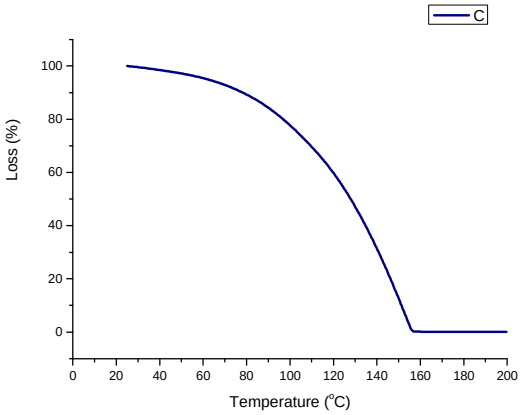

Fig. 59. Percentage loss of a AgNP + PMMA membrane

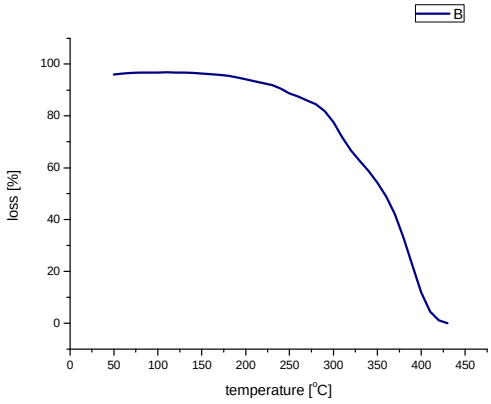

Fig. 60. Percentage loss of a AgNWs + PMMA membrane

Calculations of concentration for AgNPs + PMMA membrane were based on the TGA measurements, taking into account initial and final % weight.

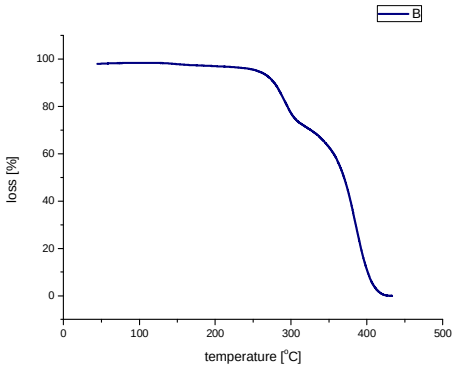

Fig. 61. Percentage loss of a TiO_2 + PMMA membrane

99,97 %- initial percentage of a membrane

0,205 %- final percentage of a membrane

$$x = \left(\frac{0{,}205}{99{,}97}\right) * 100\%$$

$$x = 0{,}205\%$$

The same calculation procedure was done for TiO_2 + PMMA and AgNWs + PMMA membranes with result equal to 0,010941% and 0,065% respectively. TGA measurements indicate the highest nanoparticle concentration in the AgNPs + PMMA membrane and the lowest in the titanium dioxide membrane. This is connected with the agglomeration tendency and coagulation at the bottom of the electrospin syringe of silver nanowires and titanium dioxide.

3.2.5. Raman spectroscopy

Raman spectroscopy technique was used in order to define the electrospun membrane components. Figures presented below show the dominating bands connected with PMMA as a membrane base. However, there are also representative peaks for silver and titanium respectively. Peak 2948 cm^{-1} corresponds to (C-H) of α-CH3 and α-CH2, peak 1720 cm^{-1} is responsible for (C=O) of (C-OO) bonds, peak 1446 cm^{-1} corresponds to (C-H) of α-CH3 and (C-H) of (O-CH3), 984 cm^{-1} is connected with the (O-CH3) bonds and 595 cm^{-1} for (C-COO) and (C-C-O) bonds [45]. Peak 2415 cm^{-1} is connected with the diamond vibration [46].

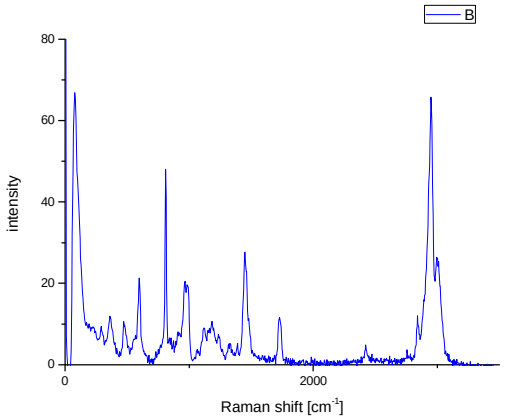

Figure 61 shows variety of peaks connected with PMMA. All the carbon related peaks were presented above nevertheless, the crucial ones are those of silver nanoparticles: 239 cm^{-1} (Ag-O) and 1057 cm^{-1} (NO_3) [42].

Fig. 62. Raman spectroscopy for silver nanoparticles incorporated into PMMA fibers

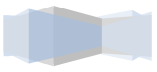

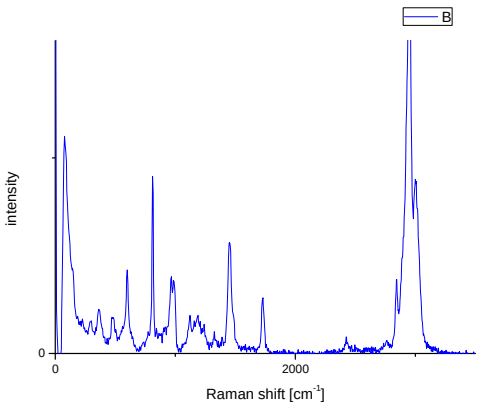

The Raman spectroscopy figure shows the dominating bands connected with poly methyl methacrylate bonds described above. What is more peaks: 370, 476 and 595 cm-1 possess typical values for titanium dioxide anatase nanoparticles [43-44]

Fig. 63. Raman spectroscopy for TiO_2 nanoparticles incorporated into PMMA fibers

3.2.6. Bacteria test

Bacteria tests of membranes were held in CIBA as in the case of nanoparticles suspensions. Figures below present the results obtained.

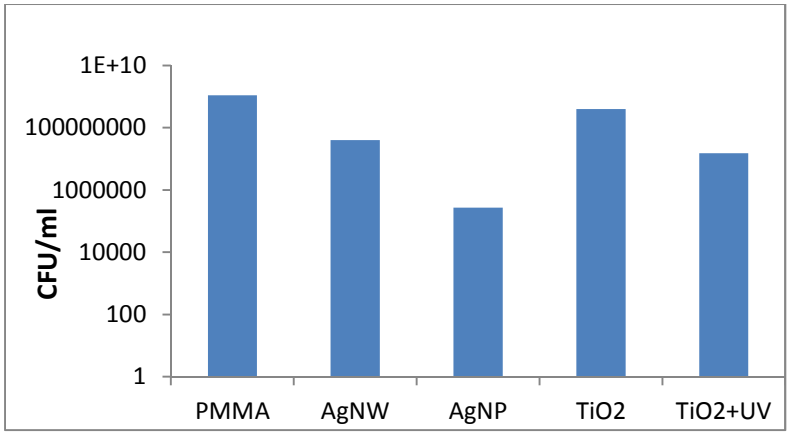

Three different membranes were examined: AgNW + PMMA, AgNP + PMMA and TiO_2 + PMMA. PMMA membrane was also examined as a control sample with no killing bacteria process being observed.

Fig. 64. Bacteria test of silver nanoparticles membrane against *S. aureus*

Moreover, TiO_2 membrane without UV illumination exhibits little bactericidal effect. The AgNP membrane has the highest bactericidal activity due, not only to the higher activity of the filler, but also due to its higher concentration in the fibers.

3.2.7. Mechanical resistance

Several measurements were carried out in order to prove the mechanical resistance of a membrane. The experimental setup was placed in the hood as it is demonstrated in the figure below. Distilled water was poured to the glass vessel and transferred through the Pall

Corporation filter holder by the CHMLAB group filter with the membrane inside. Pressure, which is an external driving force was required in order to increase the flow velocity due to high hydrophobicity of the membranes, discussed in the next section.

Fig. 65-66 Visual representation of a AgNWs + PMMA electrospun membrane and setup filtration with the membrane inside the filter holder.

Pressure and the time needed to fill 10 ml glass beaker with water were measured hence, the flow rate of a membrane was calculated. . The pressure was increased until the destruction of the membranes. AgNP + PMMA membrane was the only one which withstood until 40 kPa. Moreover, mechanical resistant of chmlab commercial membrane was measured as well and the pressure values were kept constant in order to have comparable results even if the commercial membranes was not destroyed after that pressure.

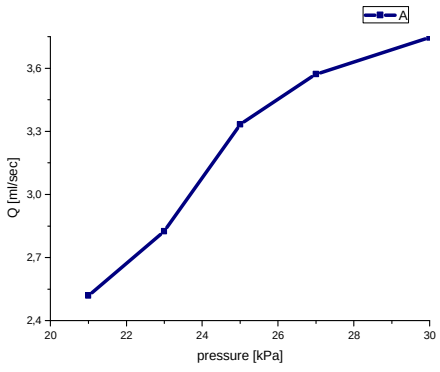

Fig. 67. Graphic representation of flux of AgNW+PMMA membrane with the maximum flux equal to 3,74 [ml/sec]

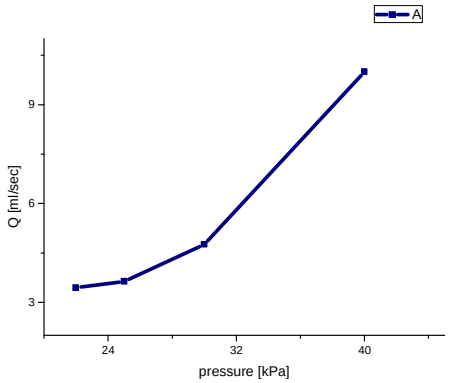

Fig. 68. Graphic representation of flux of AgNP+PMMA membrane with the maximum flux equal to 10 [ml/sec]

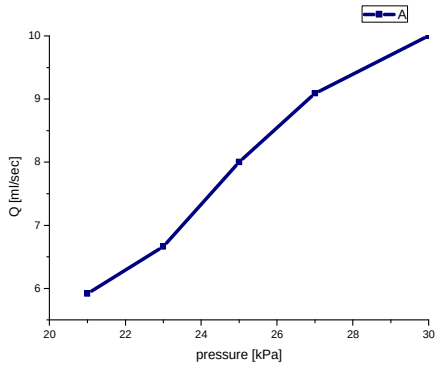

Fig. 69. Graphic representation of flux of TiO_2+PMMA membrane with the maximum flux equal to 10 [ml/sec]

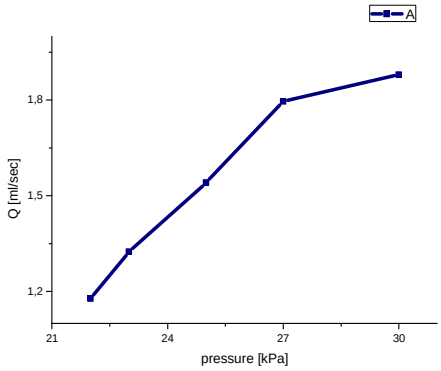

Fig. 70. Graphic representation of flux of commercial chmlab group membrane with the maximum flux equal to 1,88 [ml/sec]

The value of the flux was measured at the last available pressure, before the membrane destruction. Differences in values might be connected with high hydrophobicity of the membrane, worse particles distribution characteristic inside the polymer fibers that affect the mechanical properties. The highest flow rate was exhibited by AgNP in situ and titanium dioxide membranes probably due to the best and the most uniform particle distribution which could lead to most homogenous porosity. In the case of silver nanowires membrane where the particle distribution was not uniform, there could be a problem with agglomeration in some places so the flux was lower.

3.2.7.1.Nanoparticles stability in the membrane

During the water transfer through the membrane there was a probability of eluting nanoparticles from the polymer fibers. That is why ultraviolet visible light spectrophotometer was used in order to ensure that no nanoparticles are present in the permeate after the filtration. Results are presented in the figure below.

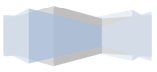

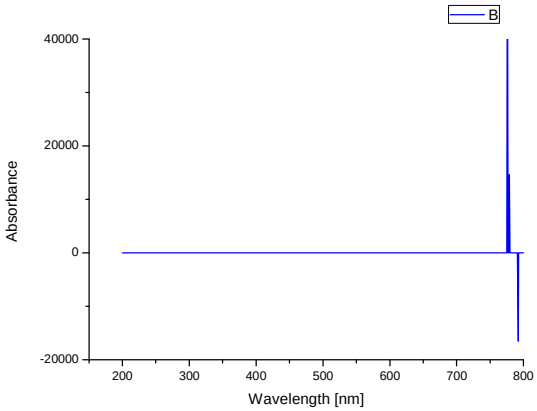

Fig. 71 UV-VIS absorption spectrum of the membrane in the water solution

Nine samples were prepared, for three kinds of membranes and at three different pressures. All the results were the same, so only one is presented in figure 70. Any characteristic peak for nanoparticles is visible, which indicates the absence of any nanoparticles in the permeate.

The same results were obtained by more accurate method called Inductively coupled plasma atomic emission spectroscopy (ICP-AES). This technique is used in order to detect trace metals. It uses inductively coupled plasma to produce excited ions and atoms that emit electromagnetic radiation with the characteristic wavelengths for a particular element. The intensity of this emission indicates the concentration of the element in the sample [18].

3.2.8. Contact angle

The contact angle measurements indicate the hydrophobicity or hydrophilicity of the material. It is an angle where a liquid/vapor interface meets a solid surface. It describes the wettability of a solid surface [18].

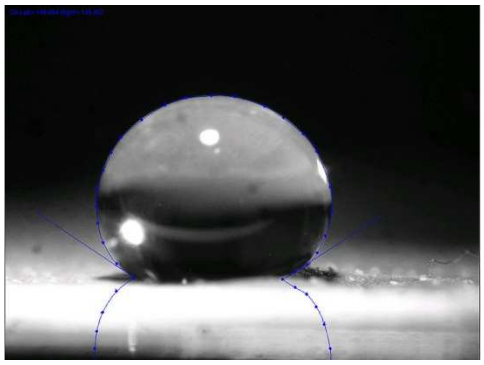

Fig. 72 An example of a contact angles measurements of water drop on a lotus leaf [18].

Values of the contact angle directly represent the properties of the material.

0^o-90^o- hydrophilic material

90^o-120^o-hydrophobic material

$>120^o$-super hydrophibic material [18]

The measurements were carried out in the Faculty of SCIENCE in the University of Zaragoza, Spain with the optical tensiometer Theta Lite 101 by Attension.

Four membranes were tested: AgNP + PMMA, AgNW + PMMA, TiO_2 + PMMA and PMMA without nanoparticles with two measurements for each. Results are presented in the table below:

AgNP+PMMA	118,47°
AgNW+PMMA	120,05°
TiO_2+PMMA	124,05°
PMMA	92,88°

Table. 12. Contact angle values for electrospun membranes

All three membranes exhibit hydrophobic or super hydrophobic properties. Control sample of PMMA without nanoparticles is hydrophobic as well but possesses lower values of contact angle. The addition of inorganic filler was already known as a method to increase the hydrophobicity of membranes [48].

4. Conclusion

The silver nanoparticles and silver nanowires were synthesized by the polyol method. The titanium dioxide nanoparticles were synthesized by the sol-gel method with the use of microwaves. Three different kinds of electrospun membranes were fabricated. Variety of characterization methods were used in order to check well distribution of nanoparticles, diameter size, bactericidal effect and mechanical resistance of membranes. The comparison to the commercial membranes were taken into account as well. Results presented in the previous sections prove the AgNP in situ method fabricated membrane being the best in terms of the most uniform nanoparticles distribution, the strongest bactericidal effect and the most mechanically resistant with the highest water flux. Titanium dioxide membrane possesses similar properties however illuminating it by UV lamp each time might be time consuming and complicated from industrial point of view and it is no effective for Gram negative bacteria. What is more, the production of silver nanoparticles in situ membrane is the cheapest among all three membranes. The production of such membranes is fast and simple. All of the three membranes are hydrophobic thanks to the membrane polymeric support and the fabrication technique. Moreover, hydrophobicity is improved by the presence of inorganic fillerssx. Thanks to the hydrophobic properties the possible fouling, swelling or fast damage of a membrane might be avoided. Water passing through the membrane will not stay inside for a long time but will elute very fast thanks to an external driving force. The comparison of the chmlab and prat dumas commercial filters were executed. Results of prat dumas

commercial filter are not presented due to improper surface behavior of the filter in the water flow with an external driving force. The future work of the project would be improving the mechanical resistance of a membrane and finding the convenient and commercial fabrication process.

5. Bibliography:

[1] Springer Handbook for Nanotechnology, Bharat Bhushan Edition, USA, 2004

[2] Silver nanoparticles: Antibacterial activity against wound isolates and *invitro* cytotoxic activity on Human Caucasian colon adenocarcinoma, J. S. Devi, B. V. Bhimba, Asian Pacific Journal of Tropical Disease, Chennai, 2012

[3] Synthesis, characterization, and evaluation of antimicrobial and cytotoxic effect of silver and titanium nanoparticles, F. Martinez-Gutierrez, P. L. Olive, A. Banuelos, E. Orrantia, N. Nino, E. Morales Sanchez, F. Ruiz, H. Bach, Y. Av-Gay, Nanomedicine: Nanotechnology, Biology, and Medicine, 2010

[4] Ag nanoparticle-embedded one-dimenshional β-CD/PVP composite nanofibers prepared via electrospinning for use in antibacterial material, S. Wang, J. Bai, C. Li, Y. Zhang, J. Zhang, China, 2012

[5] Immobilization of silver nanoparticles synthesized using Curcuma longa tuber powder and extract on cotton cloth for bactericidal activity, M. Sathishkumar, K. Sneha, Yeoung-Sang Yun, Bioresource Technology, Korea, 2010

[6] Variable frequency microwave synthesis of silver nanoparticles, Journal of Nanoparticle Research, Hongjin Jiang, Kyoung-sik Moon, Zhuqing Zhang, Suresh Pothukuchi, C.P. Wong, 2005

[7] Biofunctionalized silver nanoparticles: Advances and prospects, Colloids and Surfaces B: Biointerfaces, A.Ravindran, P.Chandran, S.Sudheer Khan, 2012

[8] Silver nanoparticles as antimicrobial agent: a case study on E. coli as a model for Gram-negative bacteria, I. Sondi, B. Salopek-Sondi, Journal of Colloid and Interface Science, Croatia, 2004

[9] Toxicity of various silver nanoparticles compared to silver ions in Daphnia magna, S. Asghari, S.A. Johari, J.H. Lee, Y.S. Kim, Y.B. Jeon, H.J. Choi, M.C. Moon, I.J. Yu, Journal of Nanobiotechnology, 2012

[10] Studies of Photokilling of bacteria using Titanium Dioxide nanoparticles, Y. H. Tsuang, J. S. Sun, Y. C. Huang, C. H. Lu, W. H. S. Chang, C. C. Wang, Taiwan, 2007

[11] Synthesis and applications of TiO_2 nanoparticles, Pakistan Engineering Congress, A.Ahmad, G.H.Awan, S.Aziz,

[12] http://dadaochem.en.made-in-china.com/product/FoVmILyOyBrv/China-Titanium-Dioxide-Anatase-Type-TiO2-98-Min-Indusreial-Grade-.html, May 2013

[13] Photocatalytic bactericidal effect of TiO_2 thin films: dynamic view of the active oxygen species responsible for the effect, Y. Kikuchi, K. Sunada, T. Iyoda, K. Hashimoto, A. Fujishima, Journal of Photochemistry and Photobiology, Japan, 1997

[14] Effects of solvents on the stability and morphology of CTAB-stabilized silver nanoparticles, Z. Khan, S. A. Al-Thabaiti, A. Y. Obaid, Z. A. Khan, A. O. Al-Youbi, Colloids and Surfaces A: Physicochemical and Engineering Aspects, India, 2011

[15] In situ photochemically assisted synthesis of silver nanoparticles in polymer matrixes, L. Balan, J.P Malval, D.J. Lougnot, France, 2010

[16] Size-controlled in situ synthesis and photo-responsive properties of silver/poly (methyl methacrylate) nanocomposite films with high silver content, C. Chen, J. Li, G. Luo, Y. Xiong, Q. Zhang, Applied surface science, China, 2012

[17] Microwave-assisted mild-temperature preparation of neodymium-doped titania for the improved photodegradation of water contaminants, Applied Catalysis A: General, V. Gomez, A. M. Balu, J. C. Serrano-Ruiz, S. Irusta, D. D. Dionysiou, R. Luque, J. Santamaria, 2012

[18] en.wikipedia.com, 2013

[19] *Staphylococcus aureus* in Rural Drinking Water, M. W. LeChevallier, R. J. Seidler, Applied and Environmental Microbiology, Oregon, 2013

[20] http://www.usawaterquality.org/volunteer/ecoli/june2008manual/chpt2_ecoli.pdf, 2013

[21]http://www.lenntech.com/applications/drinking/standards/eu-s-drinking-water-standards.htm, June 2013

[22] Antimicrobial susceptibility testing of *Neisseria meningitidis*, *Haemophilus influenzae*, and *Streptococcus pneumonia*, Centers for Disease Control and Prevention, Atlanta, 2012

[23] http://nanowatertreatment.wikispaces.com/Disk+Diffusion+Array, 2013

[24] Methods for dilution antimicrobial susceptibility tests for bacteria that grow aerobically; approved standard-seventh edition, Clinical and Laboratory Standards Institute, January 2006

[25] Introduction to membranes: Membrane selection filtration separation, Holmes Mark, Filtration+separation Journal, Elsevier, April 2007

[26]http://www.ionics.com/content/pdf/1229223-%20Lit%20Membrane%20Filtration%20Handbook.pdf, May 2013

[27] http://www.whatman.com/CelluloseAcetateMembranes.aspx, May 2013

[28] http://www.chmlab.com/index_archivos/Page1478.htm, May 2013

[29] http://www.pratdumas.com/, May 2013

[30] Convenient synthesis of silver nanowires with adjustable diameters via a solvothermal method, Journal of Colloid and Interface Science, Dapeng Chen, Xueliang Qiao, Xiaolin Qiu, Jianguo Chen, Renzhi Jiang, 2010

[31] Facile preparation of transparent and conductive polymer films based on silver nanowire/polycarbonate nanocomposite, I. Moreno, N. Navascues, M. Arruebo, S. Irusta, J. Santamaria, Nanotechnology, accepted

[32] Formation of anatase TiO_2 by microwave processing, J. N. Hart, R. Cervini, Y.-B. Cheng, G. P. Simon, L. Spiccia, Solar Energy Materials and Solar Cells, Australia 2004

[33] Microwave-assisted synthesis of silver nanoparticles using ethanol as a reducing agent, A. Pal, S. Shah, S. Devi, Materials Chemistry and Physics, India, 2009

[34] Electrospun Polyacrylonitrile/Poly(methyl methacrylate)- Derived Turbostatic Carbon Micro-/Nanotubes, Advanced Materials, E. Zussman, A .L. Yarin, A. V. Bazilevsky, R. Avrahami, M. Feldman, 2006

[35] Standard Test Method for Determining the Activity of Incorporated Antimicrobial Agent(s) In Polymeric or Hydrophobic Materials, ASTM International, Designation: E 2180-07, United States

[36] Synthesis of silver nanoparticles by chemical reduction method and their antibacterial activity, M. G. Guzman, J. Dille, S. Godet, International Journal of Chemical and Biological Engineering, 2009

[37] http://www.hindawi.com/journals/chem/2013/848205/, May 2013

[38] http://www.azom.com/article.aspx?ArticleID=3939, June 2013

[39] Raman spectrum and structure of silica aerogel, G. E. Walrafen, M. S. Hokmabadi, N. C. Holmes, W. J. Nellis, S. Henning, The Journal of Chemical Physics, 1984

[40] Thermostimulated Raman spectrum dynamics of lonsdaleite, S. Isaenko, T. Shumilova, Russia, 2012

[41] Tip- Enhanced Raman spectroscopy study of local interactions at the interface of styrene-butadiene rubber/multiwalled carbon nanotube nanocomposites, T. Suzuki, X. Yan, Y. Kitahama, H. Sato, T. Itoh, T. Miura, Y. Ozaki, Japan, 2012

[42] In-situ investigation of the formation of silver nanoparticles in polyvinyl alcohol through micro-Raman spectroscopy, K. Shadak Alee, R. Kuladeep, D. Narayana Rao, India, 2012

[43] A Raman spectroscopic study of the adsorption of fibronectin and fibrinogen on titanium dioxide nanoparticles, M. A. Strehle, P. Rosch, R. Petry, A. Hauck, R. Thull, W. Kiefer, J. Popp, Germany, 2004

[44] Raman spectra of titanium dioxide (anatase, rutile) with identified oxygen isotopes (16, 17, 18), O. Frank, M. Zukalova, B. Laskova, J. Kurti, J. Koltai, L. Kavan, Czech Republic, 2012

[45] Raman spectra of poly methyl methacrylate optical fibres excited by a 532 nm diode pumped solid state laser, K. J. Thomas, M. Sheeba, V. P. N. Nampoori, C. P. G. Vallabhan, P. Radhakrishnan, India, 2008

[46] On the origin of Raman scattering in heavily boron-doped diamond, I. I. Vlasov, E. A. Ekimov, A. A. Basov, E. Goovaerts, A. V. Zoteev, Russia

[47] Membrane for vapor/gas separation, R. W. Baker, Membrane technology and research, Inc. Canada,

[48] Optical, bactericidal and water repellent properties of electrospun nano-composite membranes of cellulose acetate and ZnO , S. Anitha, B. Brabu, D. John Thiruvadigal, et al., Carbohydrate polymers

[49] http://www.sigmaaldrich.com/spain.html, June, 2013

6. Appendix 1: Cost estimation

The comparison of the filter prices between commercial chmlab group filter and electrospun fabricated membranes were done. The table below shows the cost estimation of producing one membrane in comparison to the commercial one. The costs were based on the Sigma Aldrich prices for chemicals and the amount of ones required for the synthesis [49].

Name	Brand	Price(€)	Amount
Silver nitrate	Sigma Aldrich	89,60	25g
Ethylene glycol	Sigma Aldrich	46,40	100 mL
Polyvinylpyrrolidone	Sigma Aldrich	35,60	50g
Absolute ethanol	Sigma Aldrich	65,50	500mL
Titanium isopropoxide	Sigma Aldrich	35,30	100mL
Acetic acid	Sigma Aldrich	28,90	500mL
Poly(methyl methacrylate)	Sigma Aldrich	148,50	500MG
Acetone	Sigma Aldrich	47,80	1L

N,N-dimethyl formamide	Sigma Aldrich	121,50	1L

Table 13. List of chemicals used in the AgNP, AgNW, TiO_2 membranes synthesis with prices and amounts

Reagent	Number of possible synthesis/reagent	Price for one synthesis (€)
Silver nitrate	25/0,169=147	89,60/147=0,6
Ethylene glycol	100/20=5	46,40/5=9,28
PVP	50/0,166=299	35,60/299=0,12
PMMA	500MG/6,4=78125000	148,50/78125000=0,0000019
DMF	1/0,0018=555	121,5/555=0,22
Acetone	1/0,0012=833	47,8/833=0,06
Total price 10,28 (€)		

Table 14. Total price of AgNW + PMMA membrane production. Amounts of all the reagents required for the synthesis were taken into account.

The same calculation procedure was implemented in case of titanium dioxide and silver nanoparticles *in situ* membranes. The total price of TiO_2 membrane was 5,26 € and 0,77€ of AgNP *in situ*, which makes it the cheapest membrane.